CHEMICAL MODULATION OF SINGLET OXYGEN GENERATION RATES IN THERMAL ENDOPEROXIDE DECOMPOSITION

&

NOVEL FLUORESCENT SENSORS FOR HYPERPHOSPORYLATED TAU PROTEINS

A THESIS SUBMITTED TO
THE GRADUATE SCHOOL OF ENGINEEERING AND SCIENCE
OF BILKENT UNIVERSITY
IN PARTIAL FULLFILMENT OF THE REQUIREMENTS FOR
THE DEGREE OF
MASTER OF SCIENCE
IN
CHEMISTRY

By

Cansu Kaya

May 2016

CHEMICAL MODULATION OF SINGLET OXYGEN GENERATION RATES IN THERMAL ENDOPEROXIDE DECOMPOSITION & NOVEL FLUORESCENT SENSORS FOR HYPERPHOSPORYLATED TAU PROTEINS

By Cansu Kaya

May, 2016

We certify that we have read this thesis and that in our opinion it is fully adequate, in scope and in quality, as a thesis for the degree of Master of Science.

Engin Umut Akkaya (Advisor)

Bilge Baytekin

Salih Özçubukçu

Approved for the Graduate School of Engineering and Science:

Levent Onural

Director of the Graduate School

ABSTRACT

CHEMICAL MODULATION OF SINGLET OXYGEN GENERATION RATES IN THERMAL ENDOPEROXIDE DECOMPOSITION

&

NOVEL FLUORESCENT SENSORS FOR HYPERPHOSPORYLATED TAU PROTEINS

CANSU KAYA

M.S. in Chemistry

Supervisor: Prof. Dr. Engin Umut Akkaya

May 2016

Chemical control over singlet oxygen generation is an open to improvement because of the importance of this reactive species in biological systems. In the first project, we aimed to synthesize a silylated 1,4-dimethylnaphthalene endoperoxide derivative which is expected to release singlet oxygen on thermolysis at a relatively slow rate at room temperature. Upon the deprotection of the silyl units with fluorine ions, it is expected it to release singlet oxygen at a much higher rate, giving rise to a control over the release of the product. The absorption and the fluorescence measurement with a trap molecule which consumes the generated singlet oxygen reveals promising results for the future work for the control of singlet oxygen generation rates. In the second part of this thesis, we focused on the synthesis of a novel fluorescent sensor of a BODIPY derivative which is capable of sensing Zinc cations. The zinc complex is also expected to have a further usage for the sensing of hyperphosphorylated tau proteins, which are commonly produced in the brains of people with Alzheimer's disease. With this, it has a potential usage in the field of early detection of Alzheimer's disease.

Keywords: Singlet Oxygen, Endoperoxide, Napthalene, Absorbance, Fluorescence, Photosensitizer, Thermolysis, Chemical Modulation

ÖZET

TERMAL ENDOPEROKSİT DEKOMPOZİSYONUNDAKI ÜRETİM HIZININ KİMYASAL MODÜLASYONU

&

HİPERFOSFORİLE OLMUŞ TAU PROTEİNLERİNİ ALGILAYABİLEN ÖZGÜN FLORESAN DUYAÇLARI

CANSU KAYA

Kimya Bölümü Yüksek Lisans Tezi

Tez Yöneticisi: Prof. Dr. Engin Umut Akkaya

Mayıs 2016

Uyarılmış haldeki moleküler oksijenin (singlet oksijen) biyolojik sistemler üzerindeki önemi, bu molekülün kimyasal modülasyonla kontrollü bir şekilde üretilmesi konusundaki çalışmalara büyük bir önem kazandırmaktadır. Bu projenin ilk kısmında, sıcaklık etkisiyle kendiliğinden dekompoze olabilen ve silil gruplarıyla korunmuş 1, 4-dimetilnaftalin endoperoksitlerinin sentezlenmesi amaçlanmıştır. Florür anyonunun varlığında, deprotone olan molekülün singlet oksijen üretim hızının daha da artması ve böylelikle üretim üzerinde kimyasal modülasyonun sağlanması hedeflenmektedir. Bu amaçla, singlet oksijenle dönüşümsüz reaksiyona giren bir tuzak molekülü eşliğinde absorpsiyon ve floresans ölçümleri alınmıştır. Tezin ikinci bölümünde, floresans özelliği gösteren ve çinko katyonlarını algılayabilen Bodipy türevinin sentezlenmesi amaçlanmıştır. Çinko ile oluşturulan kompleksin, beyinde Alzheimer hastalığının bir sonucu olarak oluştuğu düşünülen hiperfosforile tau proteinlerinin tehşisinde de kullanılabilmesi hedeflenmektedir.

Anahtar Kelimeler: Singlet Oksijen, Endoperoksit, Naftalin, absorpsiyon, floresans, fotoduyarlaştırıcılar, Kimyasal Modülasyon, Termoliz

Dedicated to my Family

ACKNOWLEDGEMENT

First of all, I would like to express my sincere gratitude to my advisor Prof. Engin Umut Akkaya for his continuous support and immense knowledge of science. His patience and his guidance helped me through three years of research and writing of this thesis. He is one of a kind not only scientifically, but also as a human. I feel privileged to have had the opportunity to study in his research group and know him personally.

I would then like to thank to my thesis committee, Ass. Prof. Bilge Baytekin and Ass. Prof. Salih Özçubukçu for their presence and the fruitful scientific discussions.

Next, I would like to thank Dr. Dilek Işık Taşgın for her continuous support and help. I am really happy to know her personally. I also would like to thank Ass. Prof. Dr. Fazlı Sözmen, Dr. Tuğba Özdemir Kütük and Dr. Safacan Kölemen for their endless support throughout my senior year and my master years.

I specially thank to my fellow labmates Darika Okeev, Tuğçe Karataş, Ceren Çamur, Hale Atılgan Bila, Jose Bila, and Melek Baydar not only for the inspiring scientific discussions during our time but also for their valuable friendship through all the good times and bad times. Without them, these time interval would be meaningless. I love you all.

I would like to thank our present and past group members including Özlem Seven, Tuğçe Durgut, Nisa Yeşilgül, Esma Uçar, Yiğit Altay, Veli Polat, Deniz Yıldız, Abdurrahman Türksoy, Bilal Kılıç, Sündüs Erbaş Çakmak, Yusuf Çakmak, Onur Büyükçakır, Esra Eçik Tanrıverdi and Taha Bilal Uyar, for their support, collaborations, and friendly ambiance in the laboratory. It was a memorable journey that I had with all of them.

I thank all of my classmates of 08' including Ahmet Uçar, Kerem Emre Ercan, Lütfiye Hallıoğlu, Meryem Hatip and Sinem Gürbüz for their friendship through my years in Bilkent. I specially thank my BFF's, Aykut Aydın and Esra Soner for paving my way on chemistry with challenging discussions and for their endless valuable friendship.

I finally thank to my family; my beloved mother and father for their continuous support and unrequited love they always have for me. I thank to my two brothers and sisters in law and my nephews for always being supportive and giving me a reason to carry on. I am lucky to be the smallest member of my family for they were always leading me for the best.

LIST OF ABBREVIATIONS

BODIPY : 4, 4-difluoro-4bora-3a, 4a-diaza-s-indacene

PDT : Photodynamic Therapy

PS : Photosensitizer

DCM : Dichloromethane

DMF : Dimethylformamide

DMSO : Dimethylsulfoxide

THF : Tetrahydrofuran

DPBF : 1, 3 Diphenylisobenzofuran

TBAF : Tetra-n- butylammonium fluoride

EtOAc : Ethyl acetate

TFA : Trifluoroacetic Acid

TBDMSCl : Tertbuthyldimethyl Silyl Chloride

HOMO : Highest occupied molecular orbital

LUMO : Lowest occupied molecular orbital

ISC : Inter System Crossing

ICT : Internal Charge Transfer

PET : Photoinduced Electron Transfer

TLC : Thin Layer Chromatography

NMR : Nuclear Magnetic Resonance

MS : Mass Spectrometry

RT : Room Temperature

TABLE OF CONTENTS

LIST OF FIGURES

LIST OF TABLES

CHAPTER 1: INTRODUCTION

A. CHEMICAL MODULATION OF SINGLET OXYGEN GENERATION RATES IN THERMAL ENDOPEROXIDE DECOMPOSITION

1.1 Properties of Singlet Oxygen

1.1.1. Electronic Structure and the properties of Singlet Oxygen

Oxygen, in its ground state, is essential to all organisms and biological processes in life. Since it is highly abundant on earth, investigation on its chemistry has been going for centuries. One of the most interesting discoveries about the molecular oxygen is its powerful oxidant excited version, singlet state oxygen, which gives a variety of reactions inside biological systems. Although its discovery goes back to 1924, singlet oxygen has become the focus of the laboratory studies after the work of Khan and Kasha on chemiluminescence of the hypochlorite-peroxide reaction as caused by liberated singlet oxygen[2].

In order to understand the nature of this excited state, the electronic structure of the ground and the excited states of oxygen molecules should be investigated. Molecular oxygen ($^3\Sigma_g^-$) has two low-lying singlet excited states, above the triplet state[3]. The difference in these two states is the change in the electronic configurations of л orbitals. These are represented as delta singlet oxygen $^1\Delta_g$, which has 95 kJ /mol higher energy than ground state oxygen and sigma singlet oxygen $^1\Sigma_g^+$, which has 158 kJ /mol higher energy than the ground state oxygen[4].The latter one has a very short lifetime and is quickly converted to $^1\Delta_g$ state. $^1\Delta_g$ state has sufficient lifetime to react chemically in the biological environment[5]. These states and their corresponding orbital assignment are represented in **Figure 1.**[3]

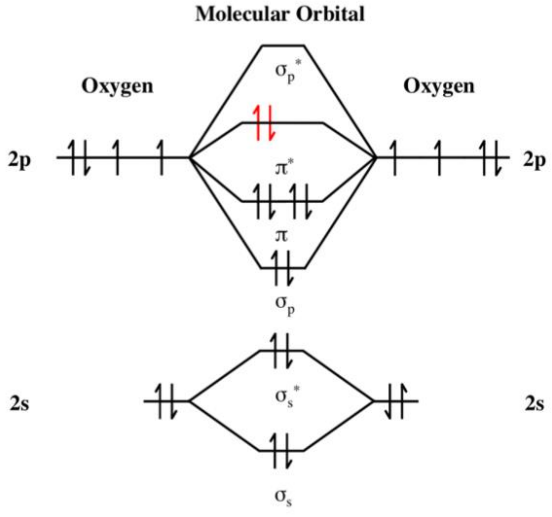

(a) $^1\Delta_g$

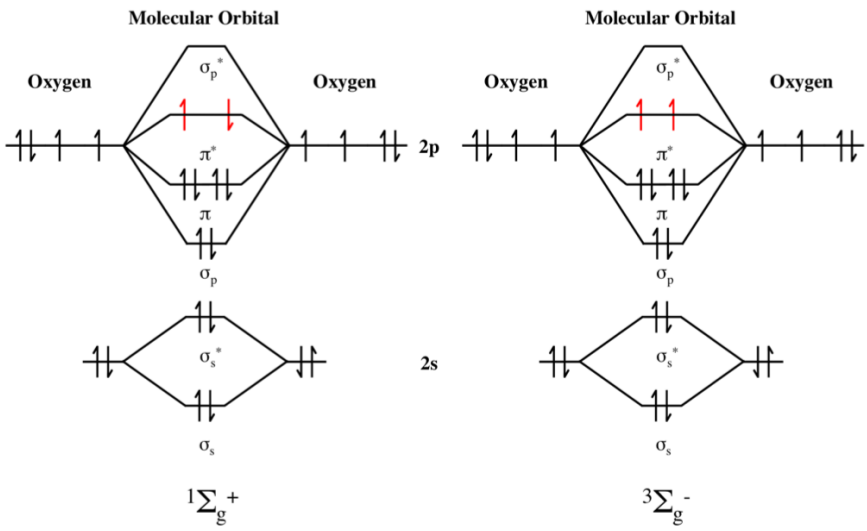

(b)

Figure 1: a) Schematic representation of $^1\Delta_g$ state of singlet state oxygen. **b)** Schematic representation of $^1\Sigma_g^+$ state of singlet oxygen and lowest triplet state of molecular oxygen.

The potential energy diagram corresponding to different energetic states of molecular oxygen can be seen in **Table 1**[3].

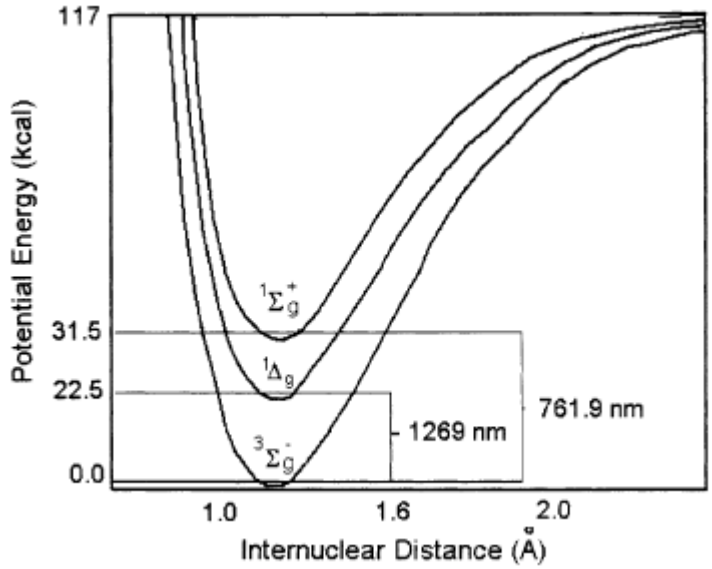

Table 1: Potential energy curves for three low lying electronic states of molecular oxygen.

Singlet oxygen is a highly reactive and short-lived intermediate and because of its highly electrophilic nature, it exhibits a high reactivity towards electron rich molecules. Since its half-life is in the range of 1-50 μs in aqueous systems, it can travel appreciable distances in the cellular environment forming allylic hydro peroxides, dioxanes and endoperoxides.

Reaction of singlet oxygen with proteins is more selective yielding some toxic products for the cell, whereas the reaction of $^1O_2$ with DNA can lead to strand breaks and formation of altered bases. Particularly, the photosensitized singlet oxygen has various applications, from photodynamic therapy to photooxidation. Like any other reactive species, it can be harmful at high concentrations, whereas at low concentration, it can act as a signaling molecule[5]. If $^1O_2$ can be selectively generated in a diseased tissue, such as tumors, it can behave as a therapeutic agent. This characteristic is most commonly used in photodynamic therapy of the cancer cells.

Recent studies on singlet oxygen also revealed that it is also involved in the cell signaling, inducing a series of genes involved in signaling cascade and initiating three different pathways[6].

1.1.2 Generation and Quenching of Singlet Oxygen

Over the years, there have been numerous methods to produce singlet oxygen for investigating its photophysichal and chemical properties. Some of the earliest investigations at the beginning of 20th century generated $^1O_2$ in a photosensitized project, such as the work by Fritzsche and Moureu, where they independently investigated the photooxygeneration of naphthalene and rubrene respectively[7]. Various ways which singlet oxygen can be generated is shown in **Figure 2**[4]**.**

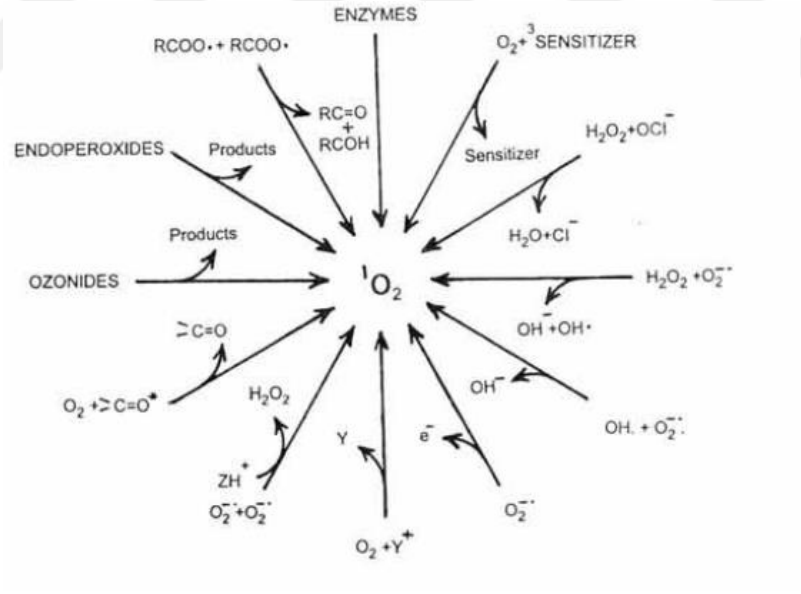

Figure 2: A schematic representation of different ways of generating oxygen.

In early 1940's, researchers began to actively investigate the chemistry of singlet oxygen and its use in organic chemistry. The very first dye sensitized photooxygenation of α–terpinene, using chlorophyll as the sensitizer, was proposed by Schenck and Ziegler to synthesize the naturally occurring trans-annular peroxide, ascaridole[8].

Dufraisse and Ecary worked with 3-diphenylisobenzofuran (DPBF), shown in **Figure 3** demonstrating its efficiency as a singlet oxygen acceptor[9]. It is today among the commonly used molecules in experiments to study the kinetics and photophysics of singlet oxygen sensitizers.

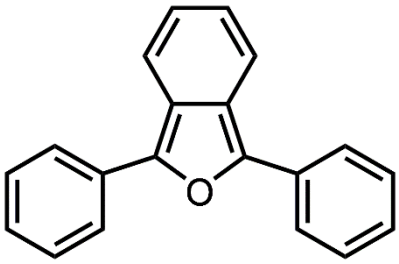

Figure 3: Structure of the commonly used singlet oxygen trap, 3-diphenylisobenzofuran.

The simplest and most controllable method for generating singlet oxygen is the photosensitized production[3]. It can be very efficient and is one of the most commonly used methods to generate $^1O_2$. This method requires only oxygen, light of an appropriate wavelength and a photosensitizer which is capable of absorbing that energy and use it to excite oxygen to its singlet state. Excitation of sensitizer is generally achieved via one photon transition (hv) between the ground state and a singlet excited state. The basic representation of this method can be seen in **Table 2**.

Currently, there is a large number of photosensitizers that are used in $^1O_2$ generation and new sensitizers are continuously being introduced. There are some specific requirements for these photosensitizers, in order to produce singlet oxygen effectively[3].

Step (a) *Absorption of light*

$$S \xrightarrow{h\nu} {}^1S$$

Step (b) *Intersystem crossing*

$${}^1S \longrightarrow {}^3S$$

Step (c) *Energy transfer from triplet excited sensitizer to ground state (triplet) oxygen.*

$${}^3S + {}^3O_2 \longrightarrow S + {}^1O_2$$

Table 2: Schematic representation of photosensitizer excitation and singlet oxygen production.

They should have a high absorption in the visible region and a triplet state of appropriate energy. The presence of a heavy atom increases the yield of intersystem crossing to the triplet state of the dye.

A high quantum yield, and a high photostability is also required. Methylene blue for example, has a strong absorption in the range of 550-770 nm and a significant quantum yield (Φ= 0.52). Some of the commonly used photosensitizers are methylene blue, fluorescein, Rose Bengal and hypericin and perylene diimide are shown together in Figure 3[10]

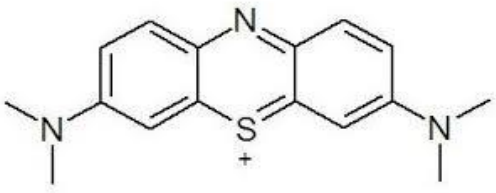

Methylene Blue

2

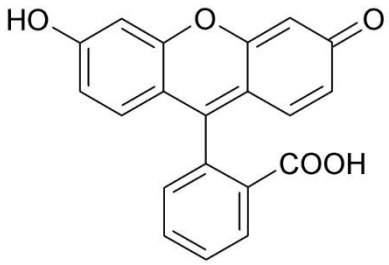

Fluorescein

3

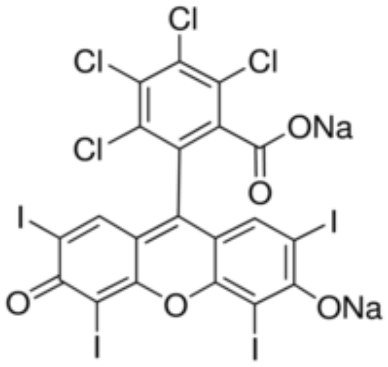

Rose Bengal

4

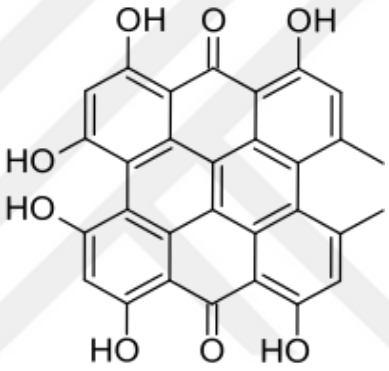

Hypericin

5

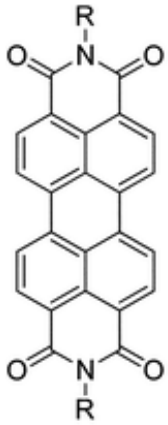

Perylenee Diimide

6

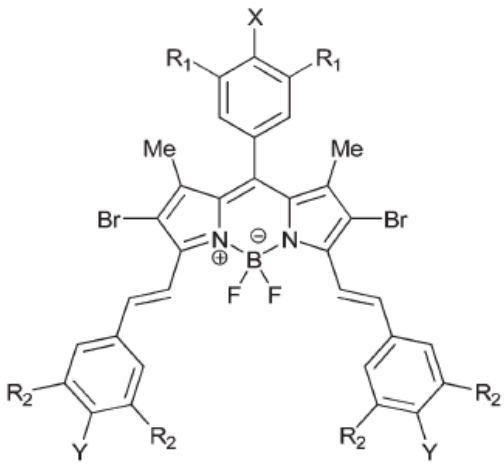

7

Figure 4: Some examples to the commonly used photosensitizer molecules.

The choice of the sensitizer is dictated by the reaction conditions such as solubility, efficiency of $^1O_2$ formation, wavelength of excitation, as well as other conditions. Recently, borrondipyromethane (BODIPY) dyes have also become attractive in this are with their high extinction coefficients and photostabilities. One example to these molecules was synthesized by Akkaya et al[11], **7**, shown in **Figure 3**. This molecule can be chemically modified and this allows attachment of chemical groups that would enable water solubility, or increase photodynamic action.

1.2 Polycyclic Aromatic Endoperoxides

1.2.1 General Information

The unique chemistry of singlet oxygen as compared to triplet ground state oxygen makes it undergo addition reactions to form endoperoxides of different types. Many polycyclic compounds can trap singlet oxygen in which they give different types of endoperoxides that exhibit different features upon warming or light irradiation. The very first observation on endoperoxides was made in 1926 by Dufrassie and his friends in which dissociation occurs with the photo oxidation of the stil unknown rubrene[12].

One of the first works on naphthalene endoperoxides was done by Wasserman et al[1], which was the synthesis 1, 4-dimethylnapthalene endoperoxide and its derivatives. Wasserman and his coworkers observed that, when two strongly electron releasing groups are present in the 1- and 4- positions of the naphthalene, endoperoxides that are generated from them were readily isolated and characterized. They also observed that, various derivatives have different half-life at different temperatures, although the decomposition of each endoperoxide yielded the original naphthalene and oxygen. The derivatives they have synthesized are shown in **Figure 5.**

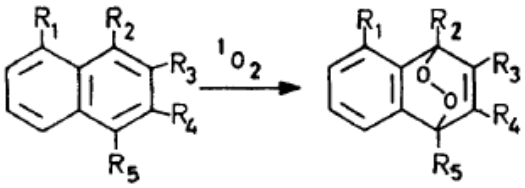

	R^1	R^2	R^3	R^4	R^5
a;	H	Me	H	H	Me
b;	Me	Me	H	H	H
c;	Me	Me	H	H	Me
d;	H	Me	Me	H	Me
e;	H	Me	Me	Me	Me

Figure 5 : Examples of suitably substituted alkyl-napthalenes[1].

After a while, this foundation is followed by the synthesis of 9,10-diphenylanthracene endoperoxide[13]. Further research revealed that at some instances, like in the case of 1, 4 dimethoxy-9, and 10-diphenylanthracene), the dissociation to produce singlet oxygen can take place at the room temperature.

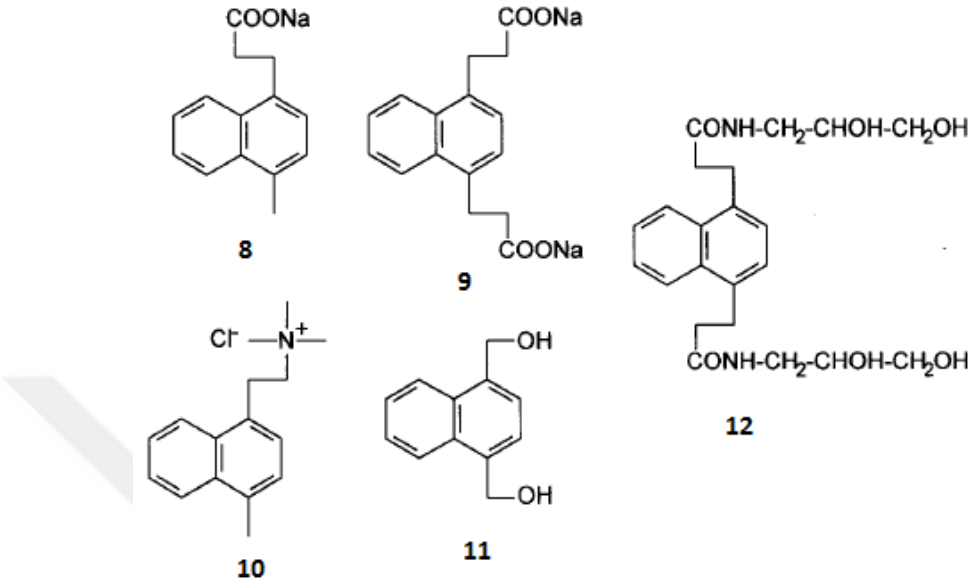

Figure 6: Syntheses of water soluble napthalene carriers of $^1O_2$.

After the observation of this new feature, water soluble naphthalene endoperoxide derivatives have been prepared and used as singled oxygen carriers as a source in biological environment by several research groups[14,15]. The very first example of water soluble carrier of singlet oxygen carries were reported by Nieuwni et al and Saito et al. These endoperoxides, shown in **Figure 6** as 8 and 9 have been used as chemical sources of singlet oxygen to assess the activity of towards biological or chemical targets.

Following these molecules, a second generation of carriers have been synthesized bearing specific groups as in the case of 10, 11 and 12. They bear some specific groups like quaternary ammonium groups or nonionic hydrophilic groups in order to assure particular affinity for specific sites[16].

All of these examples demonstrated that, with different substation patterns, it is possible to control the rate and the temperature of thermal decomposition process of polycyclic aromatic endoperoxides which provide promising application areas for decomposition of singlet oxygen.

1.2.2 Preparation of Endoperoxides

Two main classes of reaction of singlet oxygen are particularly important. First of it is the addition to olefins, which produces allylic hydroperoxides. The second one is the additions to diene systems to produce endoperoxides which are analogous to Diels-Alder reactions[17]. The latter type is most commonly referred as photosensitized oxygenation which involves [4+2] cycloaddition of singlet oxygen[18,19].

Since $^1O_2$ has a strong electrophilic nature, the reactivity of aromatic hydrocarbons towards singlet oxygen increases with increases electron donating groups involved. Thus, incorporation of groups which have high electron density on the reaction site of $^1O_2$ dramatically increases the rate constant of the addition reaction. The rate order for various groups is $H < C_6H_6 < CH_3 < OCH_3$[13]. Unsubstituted naphthalene is known to be not reacting with singlet oxygen, whereas it is possible to observe endoperoxide with 1-methyl naphthalene.

Another structural effect on reactivity is the number of fused ring. Molecules that bare more than two rings like anthracene or tetrachene showed that as the fused ring number increases, reactivity also increases about two fold[20].

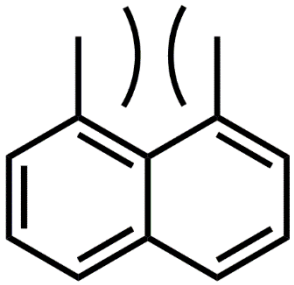

Figure 7: Steric effects on the 1, 8-dimethylnapthalene endoperoxide.

Steric effects are also important parameters which can modify the reactivity of the molecule and change regioselectivity of the cycloaddition. In the case of the molecule in **Figure 7**, interactions between two neighboring methyl groups bound to a polycyclic aromatic hydrocarbon increases its reactivity towards singlet oxygen because steric strain is relieved in the transition state. Therefore compound 13 is 4 times more reactive than the 1, 5 isomer[21].

Unlike common Diels Alder reactions, in the case of synthesis of endoperoxides from singlet oxygen, there is shown to be a strong solvent dependency of [4+2] cycloadditions. In order to understand this effect, singlet oxygen cycloaddition of 1,4 dimethylnapthalene was investigated with 28 solvents[22].

This study have revealed that the reaction rate increases 100 fold from cyclohexane to dimethylformamide, DMF and becomes even faster with water soluble analogs.

The mechanism for the cycloaddition of singlet oxygen to the aromatic compounds is very similar to the classical Diels Alder type reactions, only with little alterations. Recent studies have shown that the mechanism goes through a concerted, single step reaction, exhibiting strong charge transfer from aromatic organic donor to singlet oxygen which is demonstrated on **Figure 8**[23].

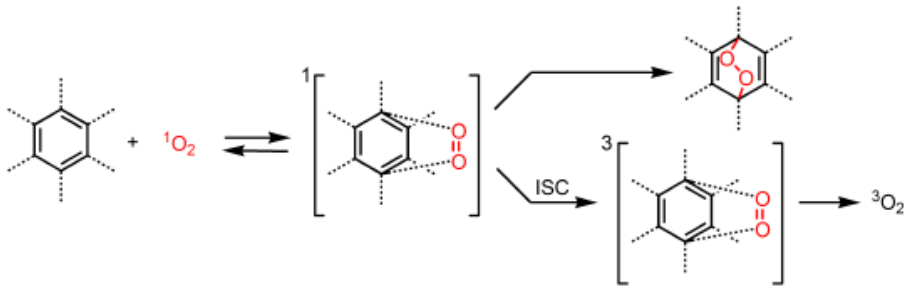

Figure 8: Mechanism of [4+2] cycloaddition of singlet oxygen on aromatic hydrocarbons.

A reversible intermediate conjugate between aromatic ring and oxygen is formed in the singlet state during the reaction. Since singlet oxygen has a highly electrophilic character, this conjugate has a highly significant charge transfer character. After the intermediate is formed, the aromatic endoperoxide can be obtained through concerted mechanism. Charge transfer mediated inter system crossing (ISC) may also take place, switching the intermediate conjugate to the triplet state and triplet oxygen to be dissociated at the end.

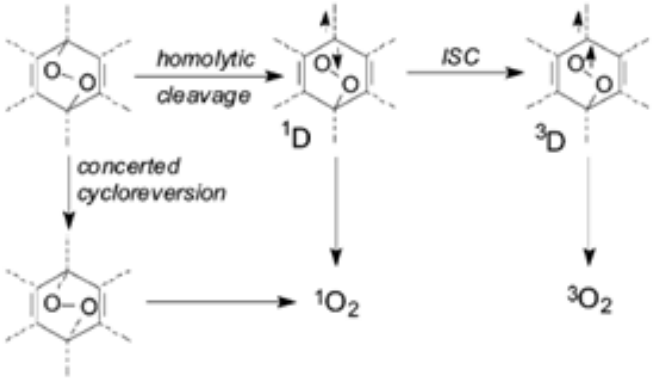

Table 3: Schematic Representation of concerted cycloreversion and homolytic cleaveage mechanisms.

Inter system crossing of singlet state oxygen to triplet state oxygen can be seen on the Jablonski diagram on **Table 3**[24]. It also shows the different electronic states of a molecule and the transitions that occur between those states.

1.2.3 Thermal Dissociation of Endoperoxides

Photolysis and thermolysis are two primary ways for endoperoxides to dissociate. Just as in photolysis, the dissociation of endoperoxides by heating involves two different mechanisms. First of them, is the cycloreversion, which leads to the substrate and molecular oxygen either in singlet or in triplet state and the cleavage of the peroxide bond. This cleaveage is often followed by rearrangements or decompositions to hydroxyketones or quinones as seen in **Figure 9**[25].

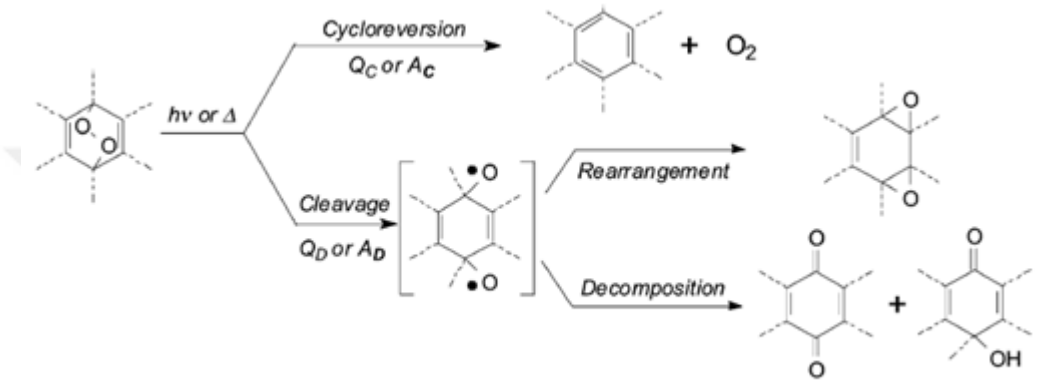

Figure 9: Thermolysis pathways for aromatic endoperoxides.

Activation enthalpy of each different endoperoxide molecule determines the ratio between cleavage and cycloreversion. In **Figure 10**, some activation parameters for the thermolysis of several aromatic endoperoxides are given[13]. It is seen that the activation enthalpy for cycloreversion, ΔH, increases from benzenic to napthalenic and 1, 4 anthracene endoperoxides. In more condensed analogues, as a result, there is a competition between cleavage and cycloreversion.

Recent work on endoperoxides revealed that the incorporation of aromatic moieties to the bridgehead position of aromatic EPO's, increases the possibility of cycloreversion process[13]. For thermal cycloversion decomposition pathway, there are also two possible mechanisms. In a concreted cycloreversion, $^1O_2$ is produced quantitatively. On the other hand, homolytic cleavage involves ISC and leads both molecular and singlet oxygen. In **Figure 10**, molecules 14, 15 and 16 are introduced by Turro and coworkers to decompose singlet oxygen in high yields, as compared to 9,10 substituted ones 17 which produce singlet and triplet state oxygen.

EndoPerOxide		$\Delta H^{\neq}$ (kJmol^{-1})	$\Delta S^{\neq}$ (JK^{-1}mol^{-1})	$^1O_2$ (%)
	**14**	74.4±2	-1.7±8	90±3
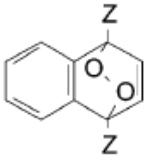	**15a**	97.0±4	0.8±5	≈100
	15b	101.1±1	8.4±4	76±1
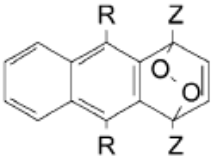	**16d**	124.6±1	-7.5±3	92±1
	16e	101.1±1	-1.3±3	95±5
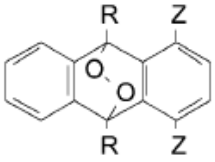	**17c**	135.8±1	40.1±2	32±1
	17d	132.9±1	30.9±3	52±4

[a] **a**: Z = H. **b**: Z = CH_3. **c**: R = C_6H_5, Z = H. **d**: R = C_6H_5, Z = CH_3. **e**: R = C_6H_5, Z = OCH_3. **f**: R = Z = C_6H_5.

Figure 10: Activation parameters for the thermolysis of various aromatic endoperoxides and corresponding singlet oxygen yields.

Further examples on naphthalene and anthracene endoperoxide derivatives are given in **Figure 11** and **Figure 12.** In addition to small molecules, polymeric endoperoxides have also been prepared as well, where naphthalene derivatives were successfully grafted on a various benzene moieties, and polymerization of methyl substituted vinylnapthalene[26]. In **Figure 11**, the temperature dependence of an anthracene endoperoxide derivative is observed by measuring the absorbance of the molecule.

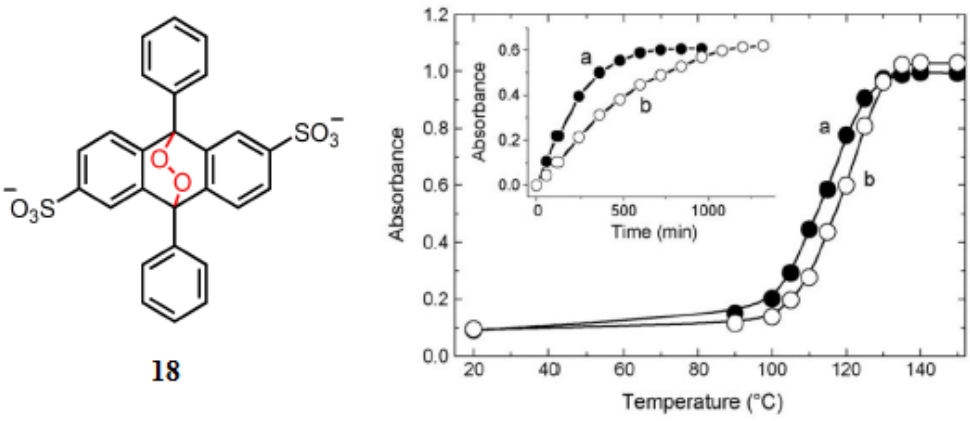

Figure 11: Temperature dependence of thermolysis of anthracene derivative. Reprinted with permission from reference 25.

In the case of **Figure 12,** although the molecule 19 is easily synthesized, its acetal structure can undergo hydrolysis in an aqueous medium[27]. The naphthalene derivative 20, however, is known to release singlet oxygen at 37 with a % 76 yield[25]. This type of molecular structure can be compatible with the biological conditions if water solubility can be attained with hydrophilic moieties.

19 **20**

Figure 12: 1-4 endoperoxide of 1-4 dimethoxy -9, 10-diphenylanthracene and 1, 4 dimethylnapthalene endoperoxide.

1.2.4 In Situ Generation and Detection of Singlet Oxygen in Cell Studies

In aqueous biological systems, photogeneration and thermal generation of singlet oxygen play important roles, such as the formation of $^1O_2$ in natural surface waters or the photodynamic effect. Since $^1O_2$ has a critical role in cell killing mechanism of photodynamic therapy, studies have focused on generating and monitoring singlet oxygen in vivo.

In order to understand whether singlet oxygen plays a key role in aforementioned reactions, it is necessary to develop a mechanism for specific detection and quantification of it. First attempts to do this were the studies made on aqueous solutions where detection can be maintained by fluorescent or near-IR phosphorescence molecules[28,29]. These molecules are most commonly known as chemical traps and they have specific properties for providing the required features.

One of the first studies on intracellular production and detection of singlet oxygen was done by Karnovsky and his coworkers, where they tried to understand whether neutrophils are producing singlet oxygen during the process of phagocytosis. For this, they coated glass beads using both water soluble 9, 10 diphenyl anthracene and perylene[30]. Since the work of Khan[2] has shown that the former molecule which is shown in **Figure 13**, gives a faster reaction rate with singlet oxygen, they were able to obtain a quantitative information about the formation of the singlet oxygen in the cells.

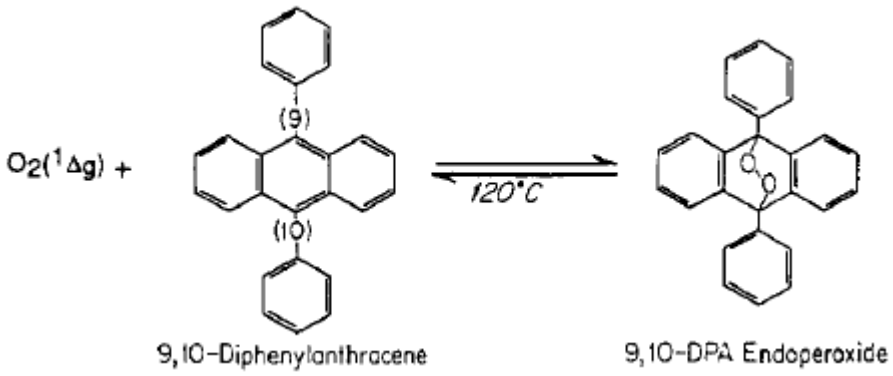

Figure 13: Reaction scheme for the9, 10 diphenyl anthracene endoperoxide.

Later, measuring the lifetime of singlet oxygen in a single cell was done by Hatz et al[31], in which single neurons and HeLa cells are subjected to time resolved optical experiments upon a photosensitizer incorporated inside them. They concluded that the lifetime of singlet oxygen in metabolically functioning, H_2O containing cells is about 3μs and this observation implies that it is best characterized as a selective reagent rather than a reactive reagent.

Investigation of singlet oxygen in vivo was further continued with the studies made on DNA. Modification of cellular DNA upon exposure to reactive oxygen was known to be the cause of induction of mutagenic oxidative stress reagents. A significant increase in the level of 8-oxo-7,8-dihydro-2'-deoxyguanosine was observed upon exposure the generation of singlet oxygen by an endoperoxide while the level of the other DNA bases remain unchanged[32].

One of the most recent studies was done in 2014, in which a potential intracellular $^1O_2$ production is observed causing the oxidation of the cellular DNA[33]. For this purpose, water soluble and thermally decomposable endoperoxide were synthesized. In order to understand the damage of singlet oxygen directly, the oxygen atom is radioactively labelled. The anthracene derivative endoperoxide that is used in the study can be seen in **Figure 14**. A cationic charge and lipophilicity of Si-DMA utilize the selective mitochondrial localization.

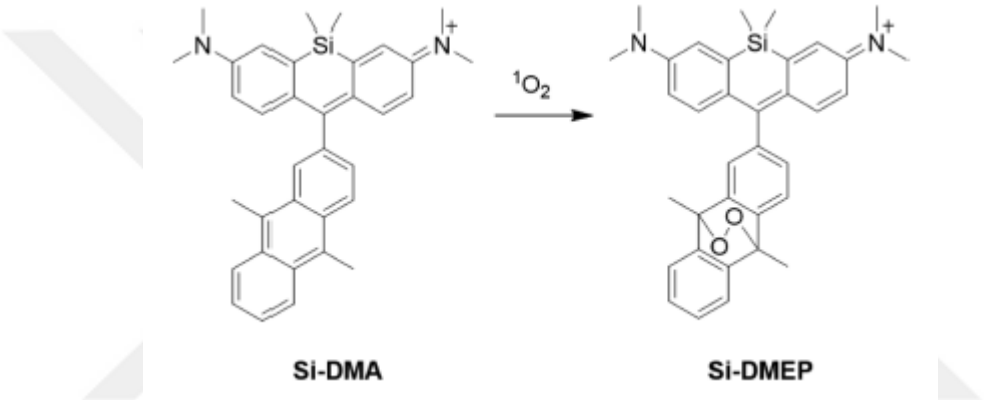

Figure 14: Structure of the Si-DMEP endoperoxide for oxidation of DNA.

1.3 Silyl Protection of Alcohols and Phenols

Many protective groups were developed to block multifunctional organic molecules for specific synthetic reactions. Various requirements, however, change the choice of protecting group depending on the site they are protecting. A protective group should not have any more functional groups to react any further than the compound to be protected. It should be easily removed, by avoiding any side products that can affect the regenerated functional group[34].

Silyl ether moieties are used most commonly for alcoholic or phenolic groups, because of their switchable reactivity on silicon atom. Among many trialkylsilyl reagents used to protect functional groups like hydroxyl groups, *tert*-butyldimethylsilyl chloride (TBDMSCl) and *tert*-butyldiphenlysilyl chloride (TBDPSCl) are the most commonly used reagents.

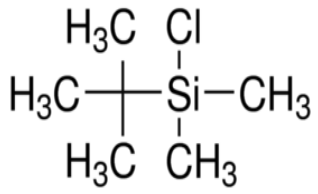

21

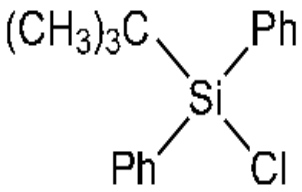

22

Figure 15: Structures of *tert*-butyldimethylsilyl chloride (21) and *tert*-butyldiphenlysilyl chloride (22).

The larger *tert*-butyl substituents disables the attack at the silicon atom, making the species a more stable substrate toward hydrolysis in weakly acidic or basic medium.

One of the properties that made silyl groups popular is the fact that they can be easily cleaved by fluoride anions. This is attributed to the fact that fluoride anion has a high affinity for silicon atom, and the Si-F bond strength is 30 kcal/mole more energetic than the Si-O bond[34,35]. There are many example usages of these protective units.

TBDMSCl was first introduced by Corey[36]. In his work, Corey showed that the dimethyl*tert*-butyl siloxy group is approximately 10^4 times more stable than trimethylsilylyl group. After this observation, solvent and the catalyst effects were further investigated, and it is found that the use of imidazole as catalyst and dimethylformamide as solvent proved to be strongly effective and provide high yields under mild conditions. The basic reaction scheme is thus shown in **Table 3.**

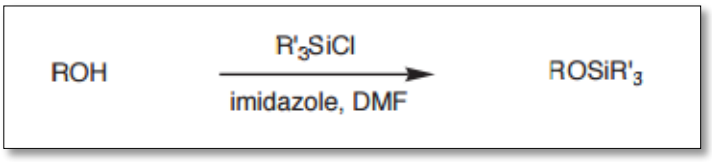

Table 4: Reaction scheme for the silylation of alcohols.

The choice of solvent, catalyst and other additional reagents for various functional groups are still under investigation. Among the various factors that influence the silylation of primary and secondary alcohols for example, the choice of solvent and catalyst are interdependent. In a 2014 study on various alcohols demonstrated that, when DMF is used as solvent, there is no need for additional catalysts because of the high catalytic activity of this solvent[37]. The structure of the alcohol and different catalysts can be seen in **Figure 16**.

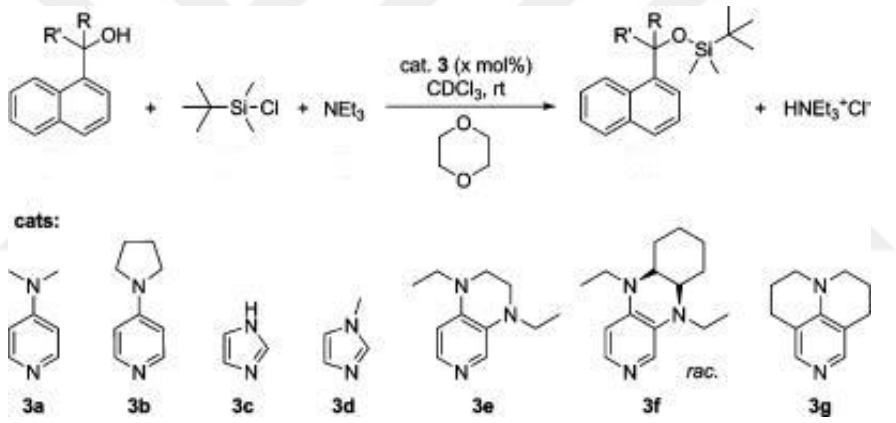

Figure 16: Silylation of various alcohols under different solvent and catalysts.

1.4 Fluorine Mediated Deprotection of Protective Groups

Anion sensing has been a great interest for many reasons. The detection of simple anions in biological systems is highly important. Different halides are distinguished by different magnitudes of binding constants or unit responses[38]. Optical sensing of fluoride anion is a challenging topic because of the high reactivity of fluoride anions in aqueous solution. They can easily be hydrated, reducing effective nuchleophilicty and basicity[39]. Since it is present enormously in organic environments, it is important to monitor its concentration.

Fluorine mediated deprotection followed by a chemical change in molecule is one of the common deprotection methods for silyl groups. In biological systems it is important to use the presence of fluoride anions for such enchaining reactions. The efficiency of this type of deprotection was investigated on various nucleic acid derivatives and it is found that it is critically dependent on the amount of water present in the TBAF molecule[40].

There are various examples in the literature, where upon deprotection with fluoride anion in the form of tetrabutylammonium fluoride (TBAF), there is a chemical process in the molecule. A recent study by Akkaya et al on a fluoride-mediated deprotection of the silyl-protecting group was investigated on a cyclic peroxide as shown in **Figure 17**[41,42] as **23**. Here, TBDMSCl protecting group was deprotected easily on addition of tetrabutylammonium fluoride, yielding a very bright blue chemiluminescence.

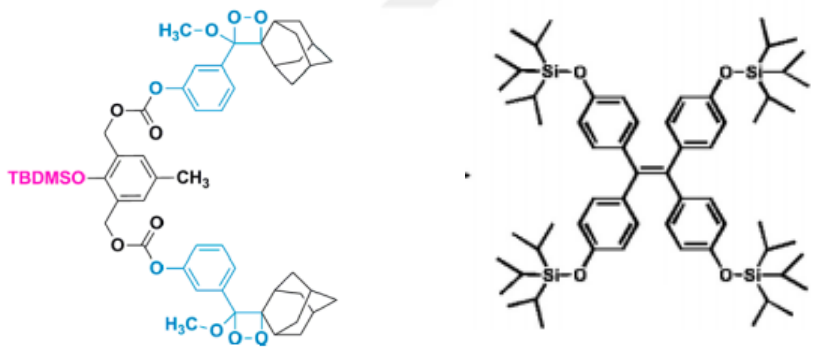

23 **24**

Figure 17: Two different examples of fluorine mediated decomposition of silyl protecting groups.

Another example of a silyl protected group is a derivative of a Tetraphenylethylene (TPE) group which is protected by four sides shown also in **Figure 17**[43] as **24**. Fluoride sensing of this molecule was accomplished by deprotection of the silyl groups from the TPE core. As a result of this, four phenoxide ions in full conjugation with the TPE moiety are available leading to a very strong intramolecular charge transfer.

B. NOVEL FLUORESCENT SENSORS FOR HYPERPHOSPORYLATED TAU PROTEINS

1.5 Supramolecular Chemistry and Molecular Recognition

Supramolecular chemistry is one of the greatest interdisciplinary fields of science. It basically focuses on the chemical, physical and biological characteristics of molecular systems that are held together by non-covalent chemical interactions. Intermolecular interactions are weaker with respect to covalent bonds. That is the reason behind the fact that the supramolecular structures are thermodynamically less stable and kinetically more labile[44].

Molecular recognition on the other hand, can be defined by the information and the energy carried by the selection of substrate by a certain receptor molecule[45]. Binding of the analyte (guest) and the receptor (host) introduces a complex or a supramolecule. As a result of this interaction, molecular information can be stored at a molecular level. In 70's, studies on selective complexation of metal ions initiated the use of notions of recognition and information which were used in relation with the biological systems[46].

Biological molecular recognition is the most complex expression of molecular recognition leading to highly selective binding, reaction and transport of the different types of molecules. Both interactional and geometrical complementary is required between the associating species. Chelating or macrocyclic ligands are often employed due to the high thermodynamic stability of the complexes that contain chelate rings.

The balance between rigidity and stability is important because binding properties may change due to these different properties. Less flexible ligands have less disorder, and macrocyclic hosts requires less solvation energy. These different properties have been used in the design of many receptors which operate through various intermolecular forces.

1.5.1 Anion and Cation Recognition

Anions and cations both play very important roles in chemistry and the biology. Although cations have attained far more interest on research for many fields, the binding characteristics of anions have not fully understood. Anionic species like fluoride, bromide or chloride have various range of geometries are known to have formed different molecular complexes[47,48].

Cation detection is very important for many biological activities. They play an important role such as enzyme activation (Zn^{2+}, Mg^{2+}, Mn^{2+}) , transmission of nerve impulses (Na^{+}, Mg^{2+}, Ca^{2+}) or regulation of the cell activity (Zn^{2+}, Mg^{2+}, Ca^{2+}) Also, detection of environmentally important cations are very important.

1.5.2 Sensors

A sensor is a device that interacts with matter or energy in order to yield a measurable signal in response[49]. Today a wide range of molecular sensors can be designed for different sensing purposes. They can signal a physical output, upon interaction with an analyte.

A molecular sensor basically is designed to have a selective interaction with different analytes. One can design a sensor that can contain binding sites that are selective and suitable for an analyte. This binding site should be able to induce a change in the signaling in terms of fluorescence emission change. There are also other designs like chemodosimer that forms a complex with a cation or anion.

1.5.3 BODIPY Dyes

4, 4-difluoro-4bora-3a, 4a-diaza-s-indacene molecule, which is most commonly known as BODIPY is first introduced by Treibs and Kreuzer in 1968[40]. BODIPY dyes and their various derivatives have wide applications from solar cells to biomolecular labelling and drug delivery systems. As previously mentioned, upon modification, these dyes are also strong candidates for photosensitizers in order to generate singlet oxygen.

The great interest on this molecules comes from their effective properties. As compared to other sensitizers, it has high fluorescence quantum yields and depending on the design, it may have high triplet quantum yields as well. Outside effects like solvent polarity or pH do not affect these molecules, therefore, they tend to maintain their structure and work in the therapeutic window. However, they can be easily decomposed under strongly acidic or basic conditions[50].

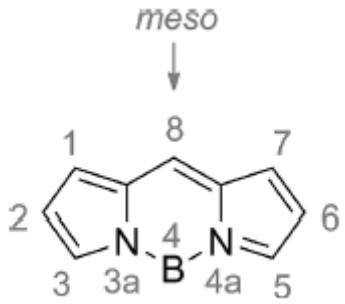

25

Figure 18: Core structure of the BODIPY dye.

A core structure of the BODIPY molecule can be seen in **Figure 18**. It can be functionalized from any different positions, from 1 to 8. This property makes it a useful candidate for functionalizing it for any purpose.

1.6 The Principles of Fluorescence and Fluorescent Chemosensors

After the excitation of a molecule by a photon with an appropriate energy, electrons follow different pathways to relax. Firstly, they scatter their energy, which is called internal conversion until the S_1 excited state. Then, from this state, they are ready to relax to the ground state via four different competitive processes[51]. These mechanisms are shown in the Jablonski Diagram which was shown in **Table 3**. Fluorescence is probably the most important of them all, where there is an emission of a photon from S_1 state to S_0. There is a difference between the absorbed and emitted energy. This is called Stokes shift. In addition to this effect, some fluorescent molecules can display further Stokes shift due to the complex formation and energy transfer[52].

A fluorophore is a molecule that emits light and fluorescent detection by fluorophore molecules is a highly sensitive, yet simple and cheap method for detecting the molecules or ions of interest. Binding of an analyte to the receptor may lead to significant changes in the photophysical properties of the fluorophore. A molecular level understanding of the biological processes in living organisms in vivo is important, because the detection of analytes in these organisms is a challenging area.

The design of the fluorescent molecular sensors have gained much attention after the work of Tsien's calcium probe in 1980's[53,54,55]. The most important property of a fluorescent sensor is to be able to detect the presence of an anion or a cation in a complex environment like cell or organism.

Fluorescent sensors that are designed for detection of cations contains two essential features. Firstly, they have a metal chelating moiety and at least one fluorophore capable of absorbing and emitting light. They may be entirely chemical or they may contain nucleic acid or peptide components[56].

Among all of the fluorescent sensors, BODIPY as a fluorescent dye, draws the greatest attention due to its unique properties. High fluorescence quantum yield, small stokes shift and high molar absorptivity makes it a great candidate for fluorescent probe. There are many examples of BODIPY based fluorescent probes in literature. Four different examples for detection of different cations are shown in **Figure 19.** Molecules 26 and 27 are specifically designed for the detection of zinc cation[57]. Molecules 28 and 29 are designed for the detection of the Cu^{+} and Cd^{2+} cations respectively[56,58]. Water soluble moieties can be attached as in the case of 27 and 29 in order to increase the hydrophilicity.

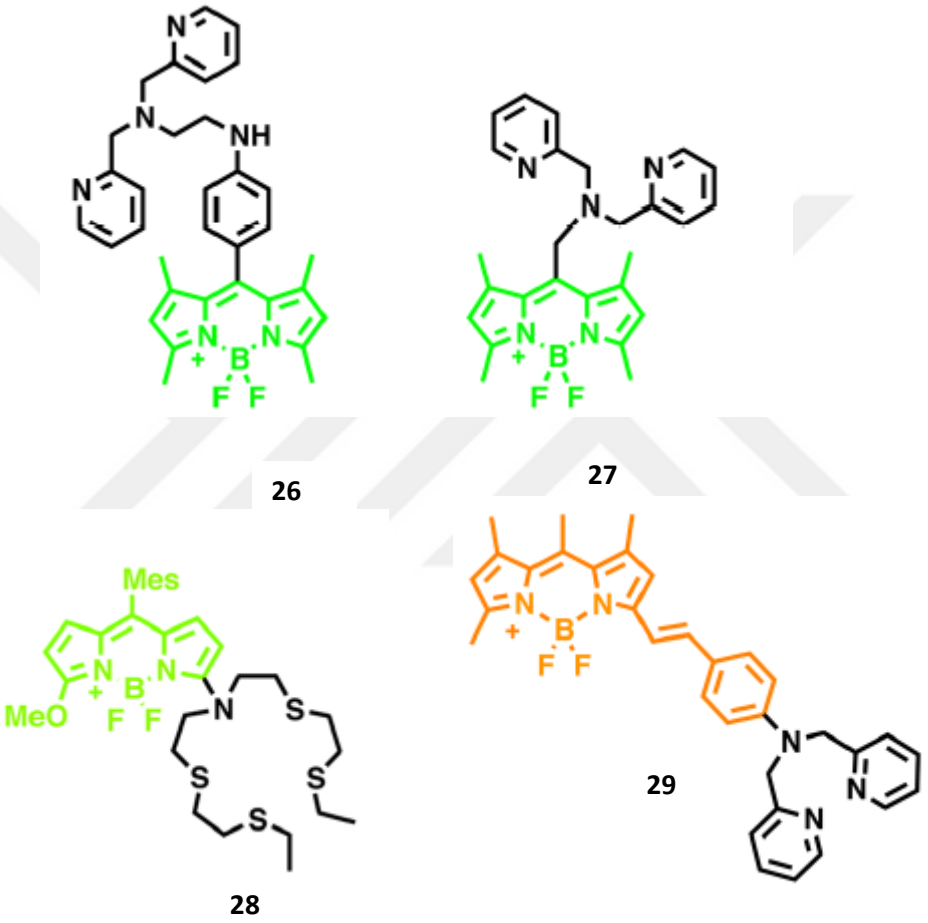

Figure 19: Examples of BODIPY based fluorescent sensors.

Further examples can be given to BODIPY based sensor with different properties. In **Figure 20**,for example, molecule 30 was introduced by Negano et al[59], has been known to have high triplet quantum yields. Molecule 31 was introduced by Hamachi and his coworkers in 2009[60]. This molecule, other than being a fluorescent Zinc sensor, has been used as molecular probe for selective detection of neurofibrially tangles in the brains of Alzheimer disease patients.

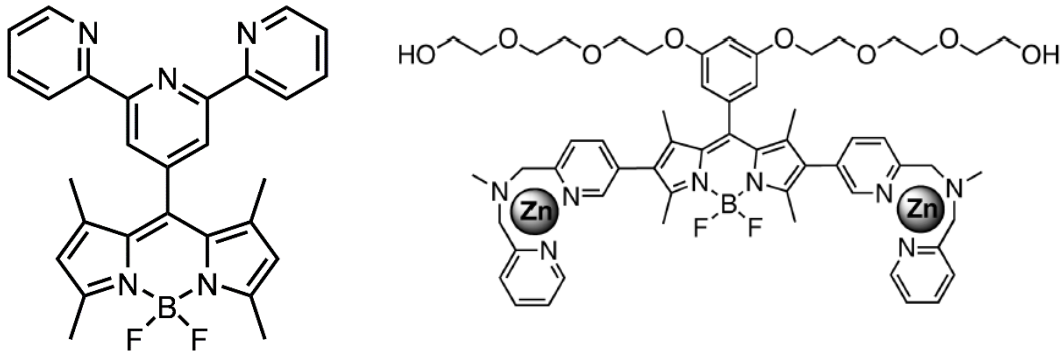

30 31

Figure 20: Some further examples to the BODIPY based sensors.

As a result of these examples, other derivatives of BODIPY molecules which can both act as a sensor and imaging probe have gained great attention.

1.7 Energy and Electron Transfer Processes

1.7.1 Photo induced Electron Transfer (PeT)

Photo induced electron transfer systems consists of three units: Fluorophore (signaling unit), receptor for recognition of an analyte, and a spacer combining these two parts. Although there is no conjugation between fluorophore and receptor in a PeT system, they are still close enough for electronic interaction by a spacer.

Firstly, an electron is excited in the PeT system, from the highest molecular orbital of the fluorophore to its lowest unoccupied molecular orbital (LUMO) upon irradiation. A receptor molecule should be able to accept and donate electrons, having its lone pair electrons at separate orbitals. When the energy of the orbital of this receptors falls between the HOMO and LUMO of the fluorophore, an electron transfer occurs from HOMO of the receptor to the HOMO of the fluorophore[61]. This occurs after the excitation process and causes an intense decrease in emission intensity together with the quenching of the fluorophore. When there is a metal cation binding to the receptor, it decreases the energy of the HOMO due to the stabilization. In this case PeT is prevented and quenching is finished.

There is also another process which is known as the reverse PeT. In this process, in the absence of an analyte, emission takes place normally. When there is an analyte such as a metal cation, the energy of the LUMO of the receptor decreases and falls within the HOMO and LUMO of the fluorophore. As a result, upon excitation electron transfer occurs between LUMO's of fluorophore and the receptor moieties. In **Figure 21**, A and B, the schematic representation of a PeT mechanism of a binding electron can be seen[62].

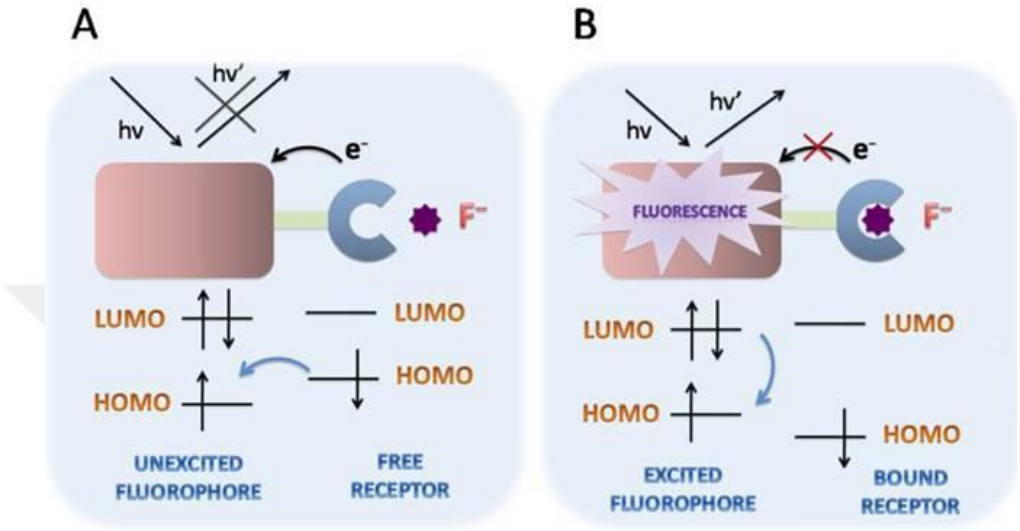

Figure 21: Schematic Representation of PeT mechanism[62].

There are many fluorescent chemosensors in the literature that work via PeT mechanism. They commonly work for cations, including H^+ and even though the molecules themselves are non-luminescent, upon binding of a cation they become fluorescent. In **Figure 22**, two different examples of sensors that work with the PeT principle can be seen[61].

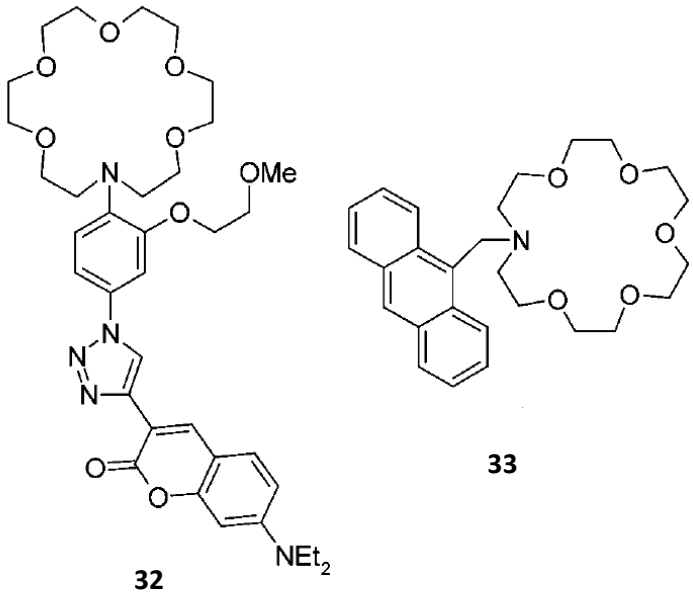

Figure 22: Examples of PeT based sensors.

1.7.2 Internal Charge transfer (ICT)

Intramolecular charge transfer is an electronic process that leads to two stokes shift in the emission spectrum a fluorescent molecule. **Blue shift** occurs when there is an electron donating group bound to the fluorophore. This decreases the ability of the electron donating group to donate, hence causing a decrease in conjugation. **Red shift** occurs when the binding group has an electron withdrawing moiety, increasing the interaction between the cation and the acceptor unit. This interaction stabilizes the excited state causing a decrease in the energy gap between HOMO and LUMO levels. The scheme that is representing these interactions can be seen on **Figure 23**[63]

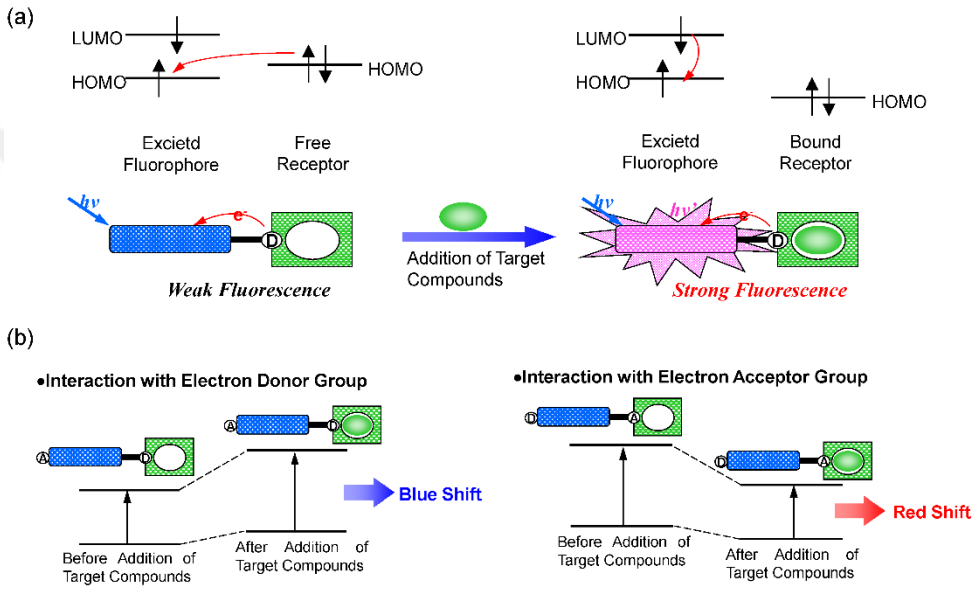

Figure 23: Schematic representation of ICT mechanism.

While designing an ICT type chemosensor, fluorophore and the receptor units are directly bound to each other and there is no spacer between them. The receptor is conjugated to the pi system of the fluorophore where it acts as an electron donor or electron acceptor according to the state of the fluorophore. This is the cause of the orbital overlapping in this conjugated system which causes the internal charge transfer.

ICT is a frequently used mechanism in the development of a fluorescent sensors. In **Figure 24,** there are two examples of molecules which give different stokes shift upon coordination with a cation[64].

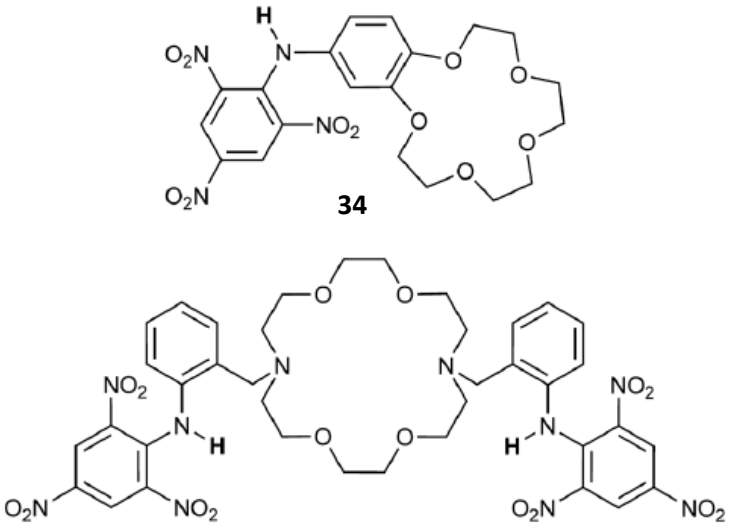

34

35

Figure 24: Some examples to ICT sensors.

CHAPTER 2: EXPERIMENTAL PROCEDURES

2.1 Methods and Materials

All chemicals and solvents are purchased from Aldrich, Merck and ABCR and were used without further purification. Merck TLC silica gel 60 F254 was used to monitor all the reactions. Column chromatography of all products was performed using Merck Silica Gel 60 (particle size: 0.040-0.063 mm, 230-400 mesh ASTM).

^{1}H-NMR and ^{1}C-NMR spectra were recorded on Bruker DPX-400 which are operating at 400 MHz for 1H-NMR and 100 MHz for ^{1}C-NMR in $CDCl_3$ and CH_3OD with TMS (tetramethylsilane) as internal standard. All spectra were recorded at 25^{o}C and coupling constants (J values) are given in Hz. Chemical shifts are given in parts per million (ppm). Splittings in the spectra are shown as s (singlet), d (doublet) t (triplet), q (quartet), m (multiplet)

Mass spectrometry measurements are conducted using Agilent Technologies 6224 TOF LC/MS devices at UNAM, Bilkent University.

Absorption and fluorescence spectrometry measurements were conducted using UV-Vis Spectrophotometer (Cary 100 Bio) and Fluorescence spectrophotometer devices at UNAM, Bilkent University.

2.2 Synthetic Pathway (1)

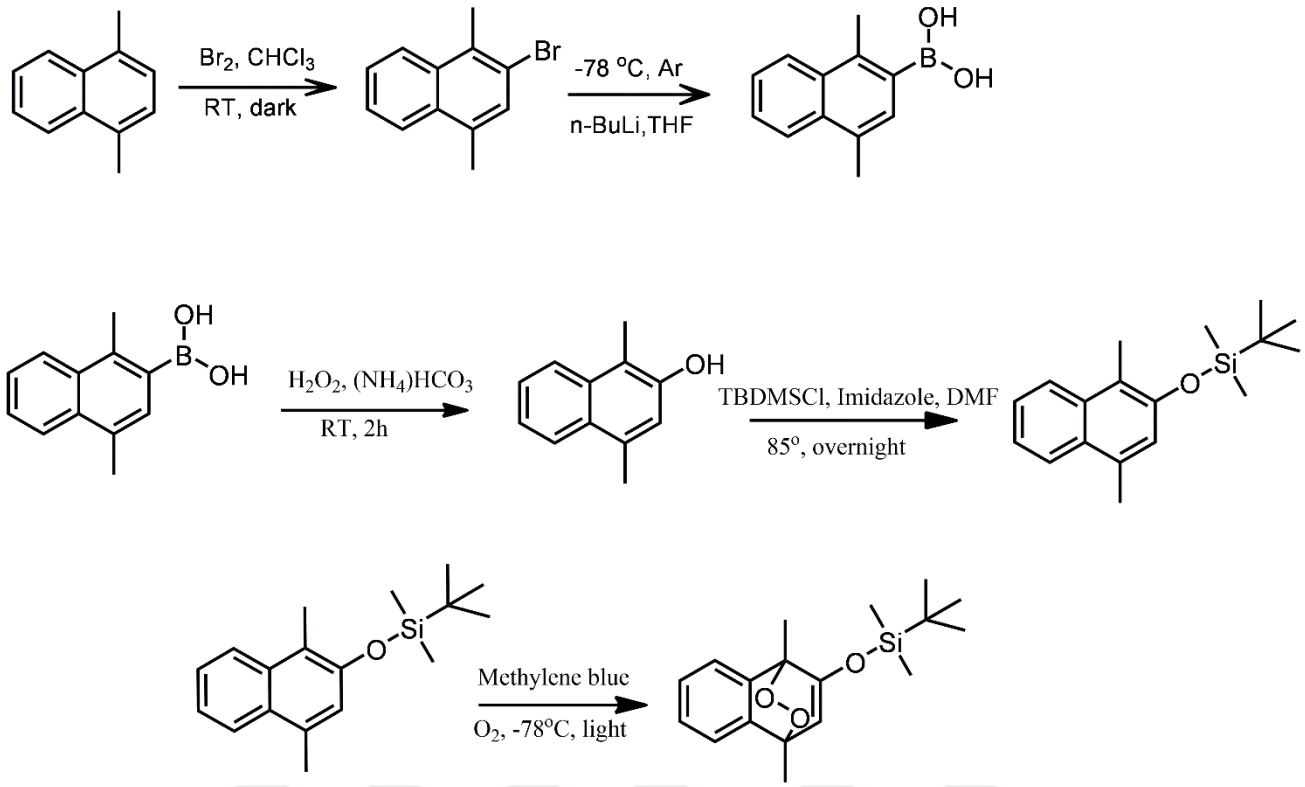

Figure 25: Synthetic Pathway for the synthesis of tert-butyl ((1,4-dimethyl-1,4-dihydro-1,4-epidioxynaphthalen-2-yl)oxy)dimethylsilane.

2.3 Synthesis of Compound 36[65]

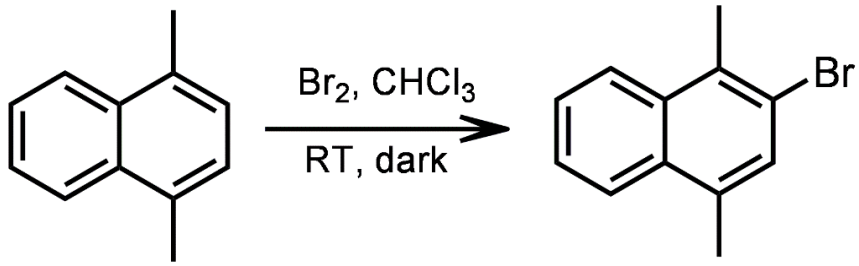

Figure 26: Synthesis of Compound 36.

1, 4 dimethyl naphthalene (1.56, 10 mmol) was dissolved in chloroform (5ml) under N_2 and exclusion of light. Bromine (1.68, 0.54 ml, 10.5 mmol) was added over a period of time (10 min) at 0° C. The reaction was warmed to room temperature and stirred for 2 hours. It was diluted with chloroform (20ml), and washed with saturated $Na_2S_2O_2$ solution (25ml), water (25 ml) and saturated NaCl solution (25 ml). The organic layer was dried over Na_2SO_4 and filtered through a thin pad of silica gel. The title compound (2.32, 99%) was used without further purification. R_f (hexane) = 0.65;

^{1}H NMR (300 MHz, $CDCl_3$) : δ 2.64 (s, 3H), 7.5 (s,1H), 7.57 (ddd, J=5.8, 4.4, *J*=32.5 Hz, 2H), 7.94-7.98 (m, 1H), 8.02-8.08 (m, 1H): ^{13}C NMR (75 MHz, $CDCl_3$): δ 18.7 (q), 19.1 (q), 122.5 (s) ,124.9 (d), 125.1 (d), 125.4 (d), 125.6 (d), 126.5 (d), 130.6 (d), 131.4 (s), 131.9 (s), 133.6 (s) 134.0 (s).

2.4 Synthesis of Compound 37[66]

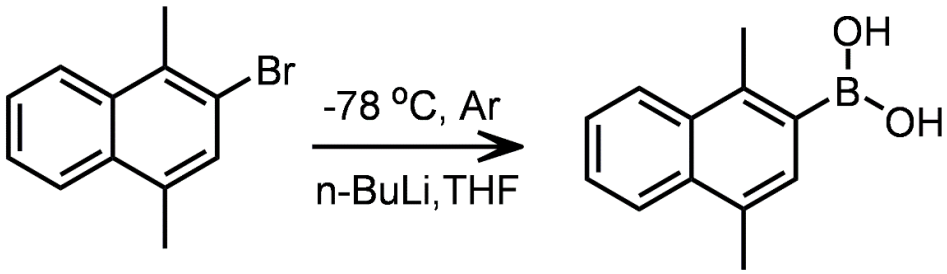

Figure 27: Synthesis of Compound 37.

To a solution of 2-bromo-1, 4 dimethyl naphthalene (2.02 g, 8.6 mmol) in dry THF, n-BuLi (2.5 M in hexanes, 7.6 ml, 18.92 mmol) was added at -78°C under N_2, and the reaction mixture was stirred for 1 hour at that temperature. Triisopropylborate (3.23 g, 3.97 g, and 17.2 mmol) was then added in one portion. The resulting mixture was stirred for 30 minutes at -78°C and at room temperature for 1 hour. It was then diluted with ether and washed with %10 HCl solution (180 ml). The ether extract was washed

with water, dried over Na_2SO_4 and the crude solid was filtered and washed with hexane to give product as a white solid. (1.45, %84)

^{1}H NMR (300 MHz, CD_3OD): δ 2.66 (s, 3H), 2.67 (s, 3H), 4.92 (s, 2H), 7.20 (s, 1H), 7.53-7.57 (m, 2H), 8.02-8.11 (m, 2H). ^{13}C NMR (100 MHz, CD3SOCD3) δ 135.29, 132.75, 132.53, 130.60, 130. 35, 125.94, 125.80, 125.12, 124.76, 19.44, 19.15

2.5 Synthesis of Compound 38[67]

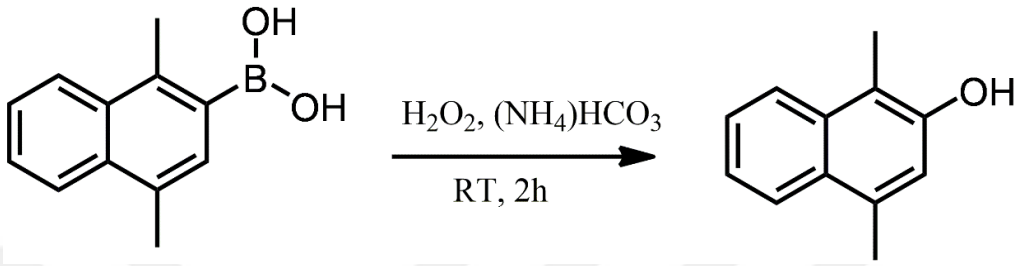

Figure 28: Synthesis of Compound 38.

%30 H_2O_2 solution (2 mmol, 0.12 ml), ammonium bicarbonate (1 mmol, 79.1 mg), allyboronic acid (1mmol), H_2O (2ml) were added to a round bottomed flask, and the reaction was performed under air at room temperature for 2 hours. After the reaction is finished, 4 ml of HCl (1 mol /L) was added to the solution till pH is 2-3. Aqueous solution is extracted with ethyl acetate (4 x5 ml), and the combined phases are dried with Na_2SO_4 to obtain the target product.

^{1}H NMR ($CDCl_3$, 400 MHz): δ 8.16 (m, 1H), 7.91 (m, 1H), 7.49 (m, 2H) , 7.09 (s,1H), 4.93 (s,1H), 2.60 (d, *J*=0.6 Hz, 3H), 2.39 (s, 3H); ^{13}C NMR ($CDCl_3$, 100 MHz) : δ 146.9, 132.1, 129.5, 126.1, 125.1, 125.0, 124.5, 124.1, 121.4, 115.7, 18.6, 15.5.

MS (TOF): m/z: Calcd; 171.09 $[M-H]^-$, found: 171. 08 $[M-H]^-$

2.6 Synthesis of Compound 39[68]

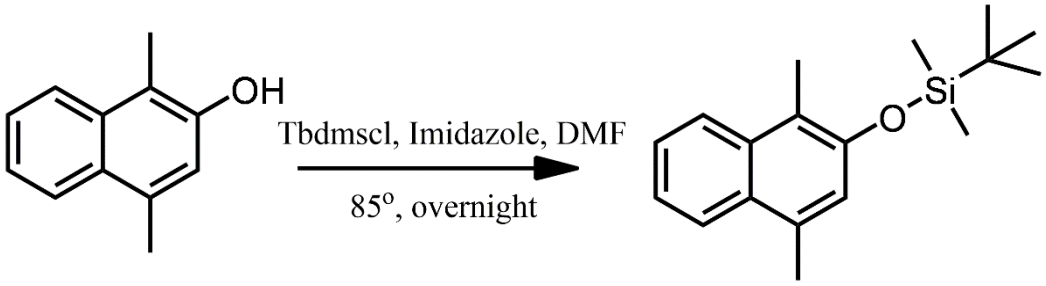

Figure 29: Synthesis of Compound 39.

1, 4-dimethylnaphthalen-2-ol (0.500 g) and imidazole (0.175 g) were added to *tert*-butyldimethylsilylchloride in 12 ml dry DMF. The mixture was stirred under argon atmosphere, at 85°-90° for 2-3 hours. The cooled mixture was extracted with dry diethyl ether.

^{1}H NMR ($CDCl_3$, 400 MHz): δ 8.11 (m, 1H), 8.01 (m, 1H), 7.49 (m, 1H), 6.62 (s,1H), 2.89 (d, *J*=0.6 Hz, 3H), 2.64 (s, 3H), 0.98 (s, 12H), 0.21 (s, 6H); ^{13}C NMR ($CDCl_3$, 100 MHz) : δ 154.3, 136.7, 133.3, 127.7,125.6, 124.1, 123.4, 120.4 30.2, 25.9, 19.9, 13.4, 0.9

MS (TOF): m/z: Calcd: 287.117 g/mol. $[M-H]^+$, Found: 287.1837 $[M-H]^+$

2.7 Synthesis of Compound 40[69]

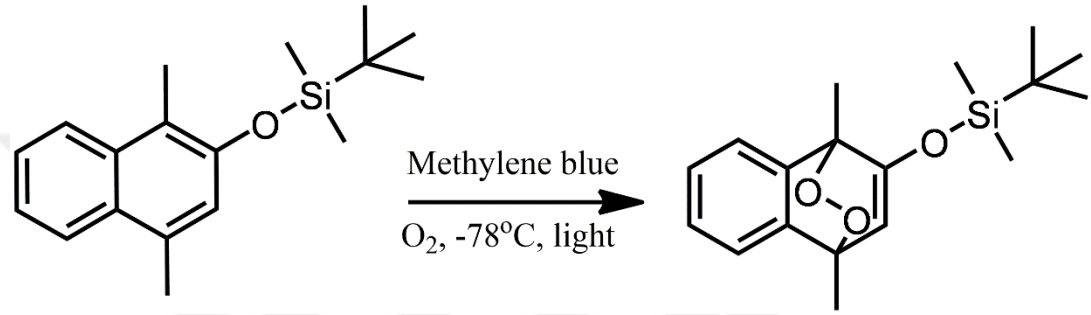

Figure 30: Synthesis of Compound 40.

Tert-butyl ((1, 4-dimethylnaphthalen-2-yl) oxy)dimethylsilane (0.100 g) was dissolved in 8 ml of chloroform. It was then added a pinch of methylene blue (approx. 2 mg) and the reaction was held under liquid nitrogen in ethanol reflux at -78°C. It was controlled with TLC (in DCM) and once the starting material was over, the solvent was removed under vacuum, without applying any external heat.

^{1}H NMR ($CDCl_3$, 400 MHz): δ 7.29 (s, J= 7.5 Hz, 2H), 7.31 (s, J= 7.5 Hz, 1H), 6.06 (s, 1H), 1.69 (s, 6H), 0.98 (s, 12 H), 0.21(s, 6 H); ^{13}C NMR ($CDCl_3$, 100 MHz) : δ 182.0, 142.7, 127.8, 121.8, 94.0, 93.1, 79.8, 31.0, 23.6, 17.1, 0.9.

2.8 Synthetic Pathway (2)

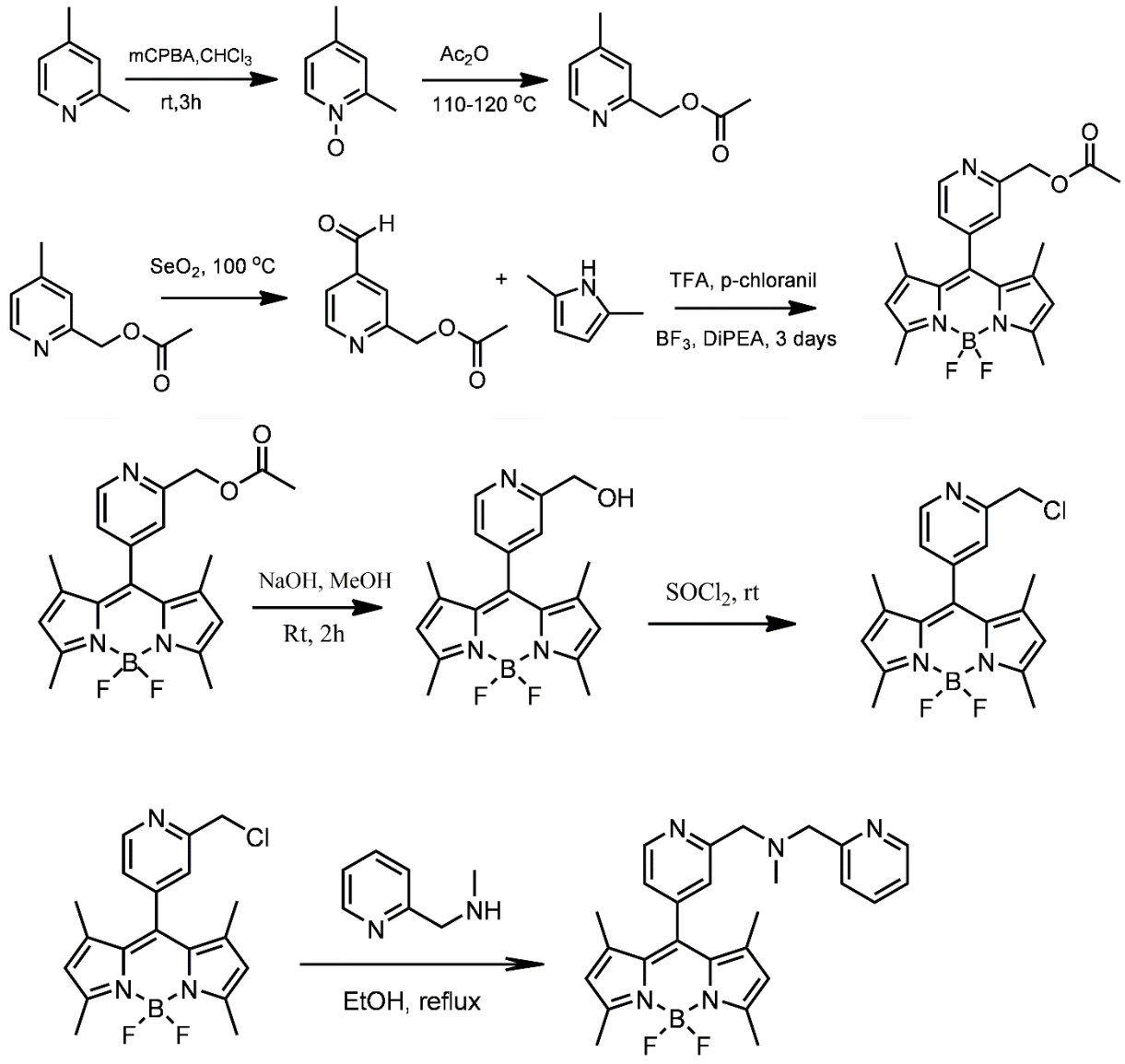

Figure 31: Schematic representation of the synthetic pathway for BODIPY based fluorescence sensor.

2.9 Synthesis of Compound 41

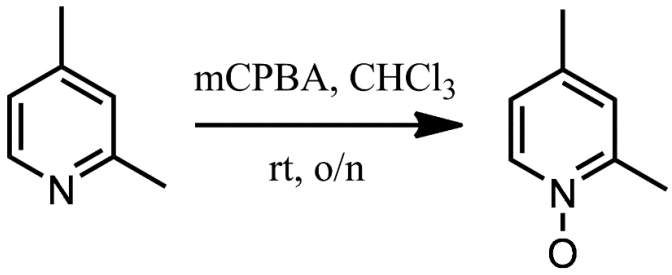

Figure 32: Synthesis of Compound 41.

In a 250 ml round bottomed flask, (5,39 g 50.3 mmol) 2,4 lutidine and (9.12 g, 52.9 mmol) mCPBA was dissolved in 125 ml chloroform. The reaction is stirred at room temperature for 3 hours. Afterwards, 4.25 g Na_2SO_3 was added to the solution. The reaction is held overnight at room temperature. To quench the reaction, 2N Na_2CO_3 solution was added. The extraction is done with $CHCl_3$ and water. The substrate is dried over K_2CO_3. ^{13}C NMR of this compound was consistent with the literature value[65].

^{1}H NMR ($CDCl_3$, 400 MHz): δ 8.33 (s, 1H), 6.94 (s, 1H), 6.87 (m, 1H), 2.49 (s, 3H), 2.26 (s, 3H); ^{13}C NMR (CDCl3, 100 MHz): δ 159.1, 149.9,147. 5, 125.3, 122.4, 21.6, 16.1.

MS (TOF): m/z: Calcd: 124.07 g/mol $[M-H]^+$, Found: 124.07 $[M-H]^+$

2.10 Synthesis of Compound 42

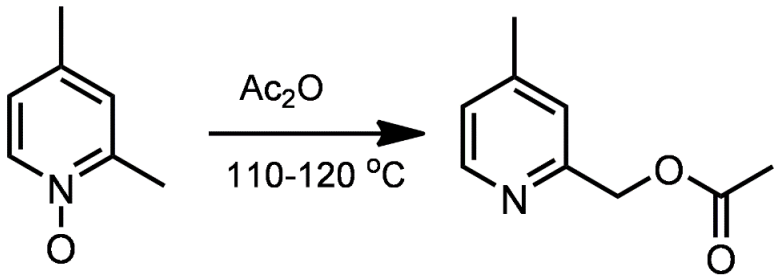

Figure 33: Synthesis of Compound 42.

Molecule was added to 5 ml of Ac_2O which is preheated to 110-120 °C. The stirring was continiued at same temperature for 30 min. 10 ml EtOH was added to the reaction and it is refluxed for 5 hours at 110 °C. The solvent Ac_2O was evaporated first, then the residue was neutralized with 2N Na_2CO_3 aqeous solution. The product was extracted with DCM and dried K_2CO_3. ^{13}C NMR of this compound was consistent with the literature value[65].

^{1}H NMR ($CDCl_3$, 400 MHz): δ 8.48 (m, J= 7.5 Hz, 1H), 7.87 (s, *J*= 7.5 Hz, 1H), 7.47 (s, *J*=1.5 Hz, 1H), 5.79 (s, *J*=7.5 Hz, 2H), 2.36 (s, 3H), 2.21(s, 3H); ^{13}C NMR ($CDCl_3$, 100 MHz) : δ 170.2, 156.2, 149.1, 147.0,122.4, 66.7, 21.6, 20.7

MS (TOF): m/z: Calcd: 166.08 g/ mol $[M-H]^+$, Found: 166.08 $[M-H]^+$

2.11 Synthesis of Compound 43

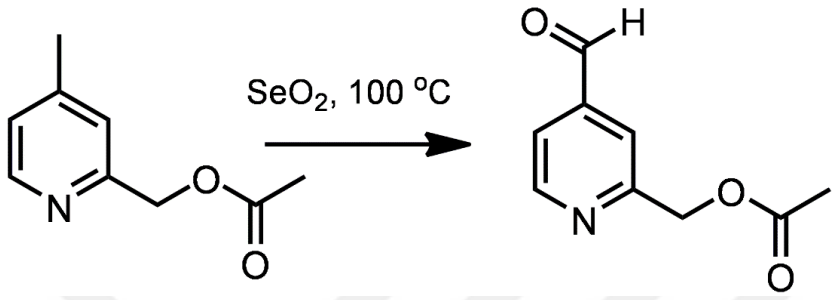

Figure 34: Synthesis of Compound 43.

0.227 g (1.60 mmol) Molecule 42 was dissolved in 50 ml of 1,4 dioxane. Then, 0.89 g (8.04 mmol) SeO_2 was added and the reaction was held under reflux at 100 °C for 3 days. It was controlled with TLC. After the starting material is consumed, the filtration was done and the product was obtained after the evaporation of the solvent.

^{1}H NMR ($CDCl_3$, 400 MHz): δ 9.60 (s, 1H), 8.94 (s, *J*= 7.5 Hz, H), 8.33 (s, *J*= 7.5 Hz, 1H), 7.66 (s, *J*= 7.5 Hz 1H), 5.78 (s, 2H), 2.21 (s, 3H); ^{13}C NMR (CDCl3, 100 MHz) δ191.0, 170.2, 141.7,136. 3, 132.9, 129.4, 128.8, 128.2, 66.1, 20.7.

2.12 Syntesis of Compound 44[70]

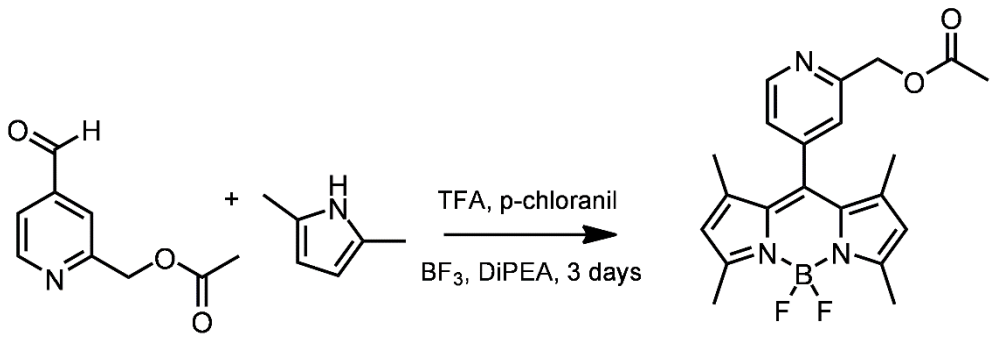

Figure 35: Synthesis of Compound 44.

1,4 dimethyl pyrolle (0.382 ml, 3.71mmol) and (0.266 g, 1.48 mmol) molecule .. was dissolved in DCM under Ar. 1-2 drops of TFA was added and the reaction was stirred at room temperature for 3 days. DiPEA (1,5 ml) and p-chloranil(0.365 g) was added and the reaction was stirred for 1 hour. After, BF_3 was added and the reaction was stirred for 1 more day. The dark precipitate was filtered off, and it was reduced under vacuum and d to give the product.

^{1}H NMR ($CDCl_3$, 400 MHz): δ 8.59 (m, *J*=7.5 Hz, 1H), 7.88 (m *J*=1.5 Hz, 1H), 7.21 (s, *J*=7.5 Hz, 1H), 5.80 (1H), 5.79 (s, *J*=1.5 Hz, 2H), 5.17(1H) , 2.72 (3H), 2.59(3H), 2.21(3H), 1.87 (3H), 1.49 (3H) ^{13}C NMR (CDCl3, 100 MHz) : δ 170.2, 156.1, 148.9, 148.0, 144.6, 143.6, 137.7, 127.8, 129.3, 131.7, 124.4, 118.7, 116.2, 113.5, 107.4, 66.8, 19.5.

MS (TOF): m/z: Calcd: 398.18 g/mol $[M-H]^+$, Found: 398.08 $[M-H]^+$

CHAPTER 3: RESULTS AND DISCUSSION

A) CHEMICAL MODULATION OF SINGLET OXYGEN GENERATION RATES IN THERMAL ENDOPEROXIDE DECOMPOSITION

Singlet oxygen production in biological systems either thermolysis or photolysis of endoperoxides is a challenging area. The chemical modulation of thermolysis is important because it enables the potential control of singlet oxygen release rate in cells. There is a wide range of examples of different types of endoperoxides and each of them has a specific quality that is required for the purpose of use. Anthracenic and napthalenic derivatives are very common because of the ease of the synthesis and isolation of these molecules and their unique properties upon formation of the endoperoxides.

In our first project, we aimed to synthesize a novel naphthalene based endoperoxide, which can release singlet oxygen either itself or in the presence of a fluoride anion. We wanted to have a structure which when protected, releases singlet oxygen in a slow rate, whereas upon deprotection, releases the singlet oxygen with a relatively faster rate. For this purpose, the starting material that is chosen was 1, 4 -dimethylnaphthalene on **Figure 36**.

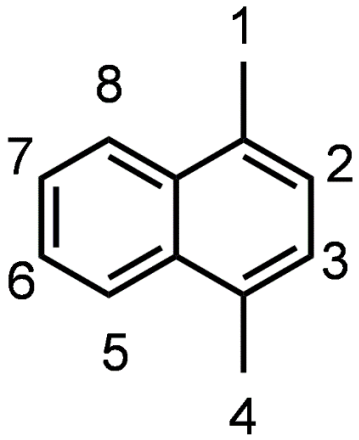

Figure 36: Structure of the 1, 4-dimethylnapthalene ring.

It was previously shown in literature that even though naphthalene itself did not readily react to give endoperoxides, the electron donating substituents on the molecule increased its reactivity towards the [4+2] addition reaction. In order to achieve this, we functionalized the core from the second position with a *tert*-butyldimethylsilyl (TBDMSCl) group. This moiety, due its bulky nature and electronic properties, have increased the ability of our molecule to form an endoperoxide.

For the functionalization of the 1, 4 dimethylnapthalene ring, bromination followed by boronic acid synthesis was conducted on the C-3 position of the ring. Bromination reaction was held under room temperature at given conditons. The resulting structure was identified by the ^{1}H-NMR peak on **Figure 28** via the change in the aromatic ring peaks on C-6, 7 and C-5, 8 together with the proton on the C-4 position. The shift of this proton moves to downfield from 7.17 ppm to 7.65 ppm.

Boronic acid transformation on the same position was done under -78 ^{0}C with dry ice at the conditions given in figure 20. The ^{1}H NMR on **Figure 29** shows the change of the same proton on C-4 position from 7.65 ppm to 7.25 ppm. Boronic acid moiety gives a high yield reaction to phenol in the presence of hydrogen peroxide and water with the catalysis of ammonium monohydrate chloride. The presence of hydroxide group on the ring can be identified by the broad peak at around 5.00 ppm and the high field shift at the C-4 proton to around 6.62 ppm. Also, the mass spectrum of the compound gives the expected mass at M^{-} as 171.34 g/mole.

After the formation of phenolic moiety, TBDMSCl protection was conducted for the formation of the molecule 28. Since the tertbutyl and the methyl both have a sharp distinct peak at around 0.98 ppm and 0.20 ppm, the molecule is easily identified, and it was further put on the reaction to give endoperoxide.

Singlet oxygen production followed by endoperoxide formation was held in chloroform in -78 ^{0}C which is maintained by ethanol circulation under liquid nitrogen. As a photosensitizer, we used methylene blue, since it has a high quantum yield and easy to remove once the reaction is finished. As a light source, we used a 500 W halogen lamp in the wide range. Singlet oxygen addition mechanism to 1, 4-dimethylnaphthalene is shown on **Figure 37**. The endoperoxide formation was confirmed by the distinct peak of the 4th proton at around 5.50 ppm. This shift is due to combination of the presence of electron withdrawing effect of the oxygens on the ring and the steric effects of the siloxy group.

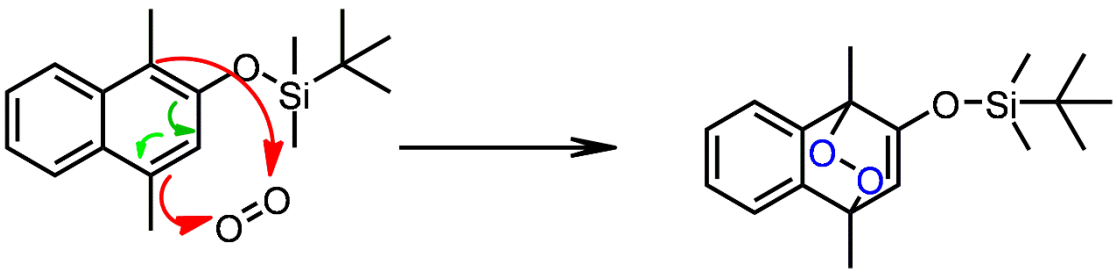

Figure 37: The [4+2] addition reaction of singlet oxygen to molecule 28.

After the formation of the endoperoxide, the absorption measurements were taken under the following conditions. The endoperoxide is dissolved in DMSO which has been held through Ar. The concentration of the endoperoxide solution was set to 35 μM. As a trap molecule, 1, 3 diphenylisobenzofuran (DPBF) was used. The concentration of trap molecule was set to 400 μM. First, as a control experiment, absorption of the trap solution alone was monitored for 5 minutes in the dark, in order to set absorption of it to 1.

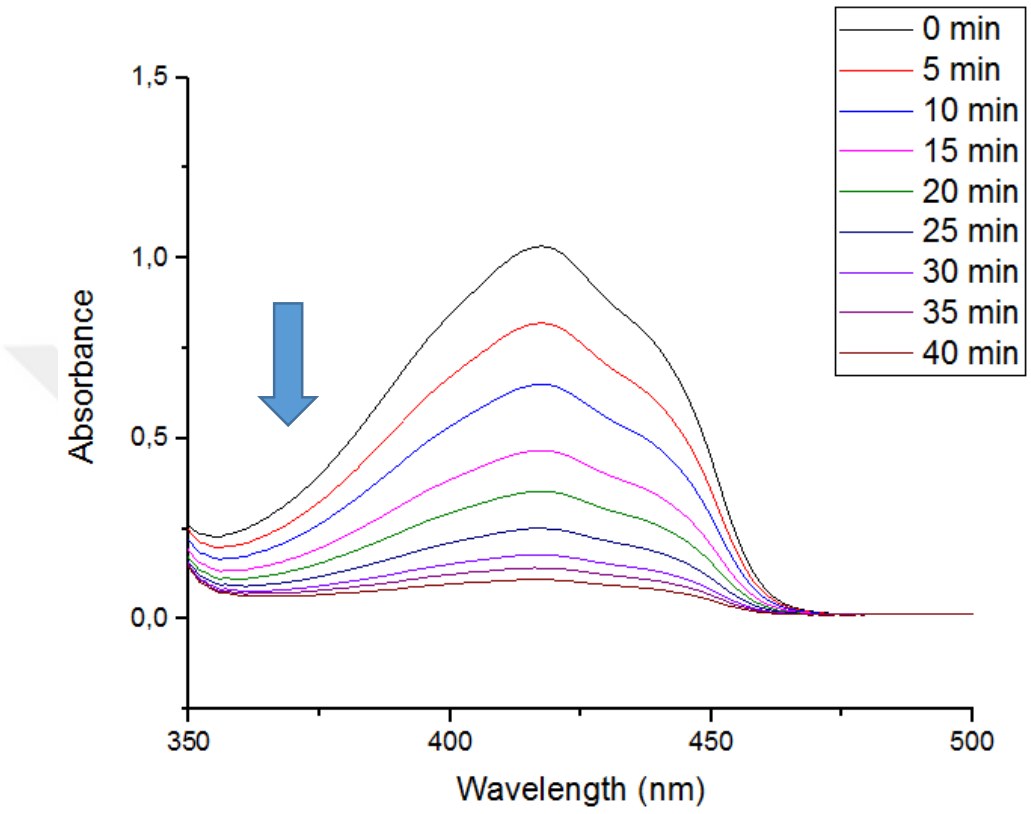

Figure 38: Absorption spectra of the Molecule 29.

After the synthesis and purification of the endoperoxide, a mixture of trap solution and the endoperoxide solution was monitored for 40 minutes at intervals of 5 minutes in the dark.

The absorption spectrum was measured between 300-500 nm, in the more energetic blue region of the spectrum. As it is shown on **Figure 38,** each color on the spectra corresponds to a different absorption value for each minute of measurement. The absorbance value of the endoperoxide falls from 1 to 0 as the time passes from 0 to 40 minutes for molecule 29. This result show that our molecule is able to produce singlet oxygen at slow rate at room temperature.

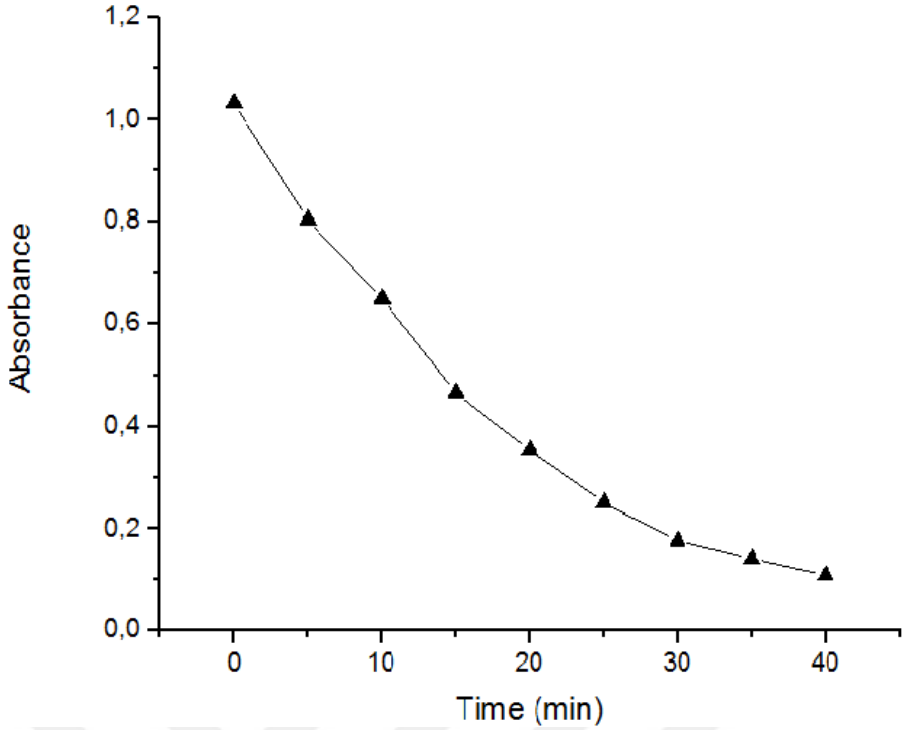

Figure 39: Absorption Change (abs) versus time (min) graph of the singlet oxygen release.

The change of absorbance within time is shown in another graph on **Figure 39**. There is a distinct decrease on the absorption within 40 minutes of measurement. This promotes our first data on Figure 26. The absorption value drops up to 0 after 40 minutes.

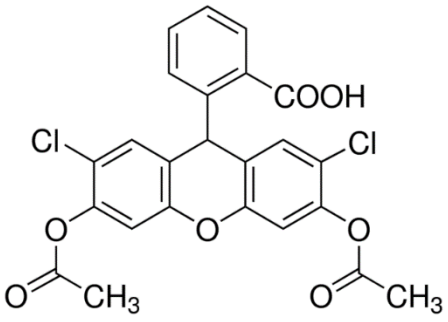

45

Figure 40: Structure of 2', 7'- dichlorofluorescein.

For the further investigation of the singlet oxygen generation upon deprotection of our molecule 29, we prepared a tetrabutylammonium fluoride (TBAF) solution in DMSO, with a concentration of 1.5 mM. Since it is previously discussed, this molecule is commonly used in fluorine mediated deprotonation reactions for it is easily prepared and stored. As a trap molecule, this time, we chose 2', 7'- dichlorofluorescein which is hydrolyzed prior to usage. The structure of it can be seen in **Figure 40.**

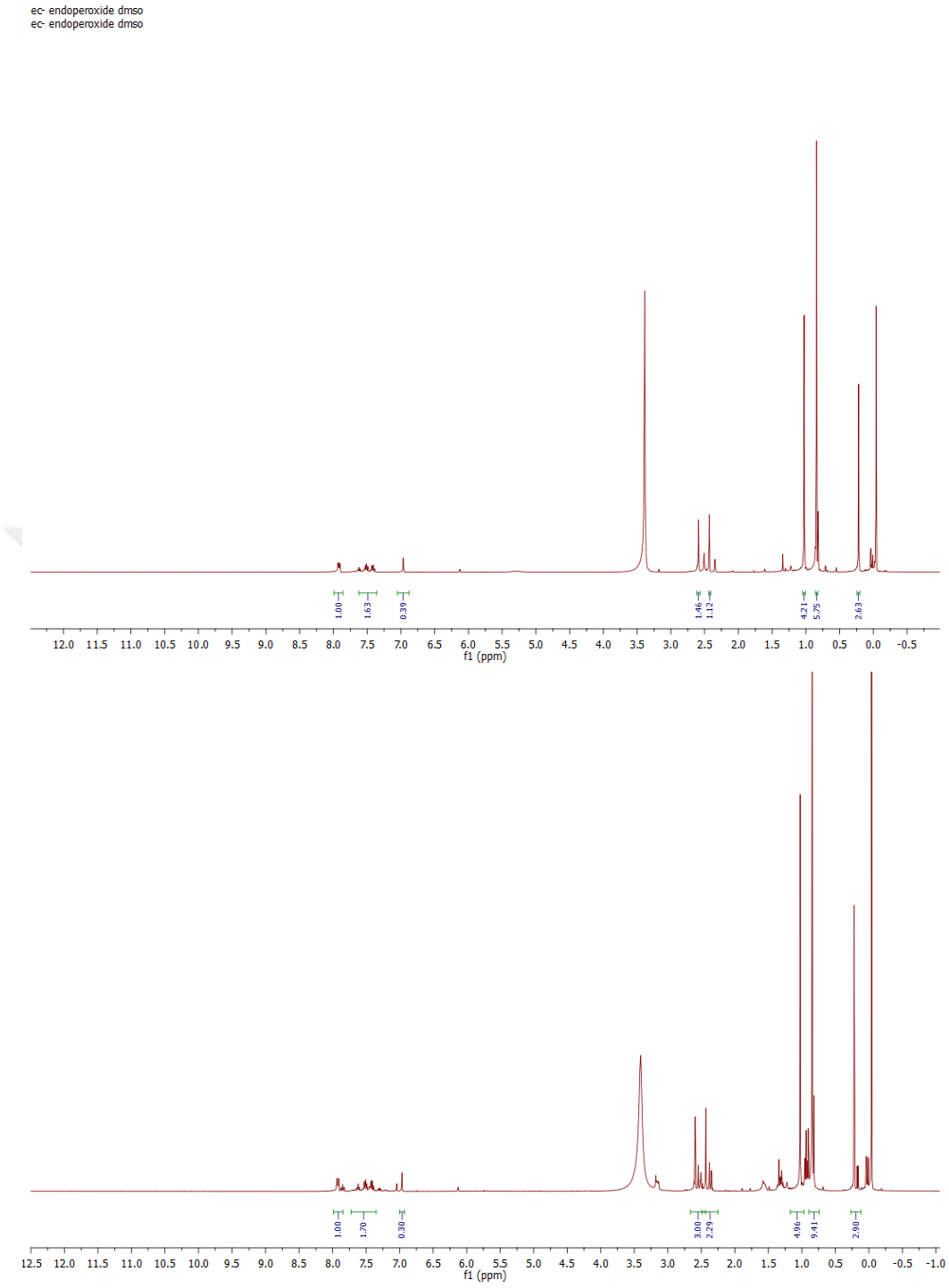

Table 5: ^{1}H-NMR of Endoperoxide in $(CD_3)_2SO$ without (top) and with (down) tetrabutylammonium fluoride.

The reason for choosing this molecule was to observe the change in singlet oxygen release via fluorescence, rather than the absorbance measurements.

For further investigation, we have identified the changes in the ^{1}H-NMR spectra of our endoperoxide upon addition of the fluoride anion. The first spectra in **Figure 51** was taken in deuterated DMSO, $(CD_3)_2$ SO. Afterwards, a pinch of tetrabutylammonium fluoride was added and the ^{1}H-NMR spectra was taken again. It is shown in **Figure 52.** These two spectra can be seen on Table 5.

Since the thermal decomposition of our endoperoxide occurs at room temperature, by looking at Table 5, we can say that during the purification, some of the molecule has already been decomposed. Upon addition of fluorine anion, although the shifts and the integral values are not changed dramatically, there is a significant decrease in the intensity of the peaks. As the fluorine atom deprotects our molecule, the mixture that we take the spectra is possibly a combination of the Molecule 38 and Molecule 39. A decrease in the aliphatic region intensities is due to the fact that some of the molecule 39 is deprotected and produced the hydroxyl moiety on the C-2 carbon, yielding molecule 38.

B) NOVEL FLUORESCENT SENSORS FOR HYPERPHOSPORYLATED TAU PROTEINS

It is important to define the chemical form or the specification of the metal ions in biological samples. Fluorescent sensors are therefore designed to measure those accessible or labile metal ions. After the first measurement of a transition metal ion Zn^{2+} was done by Zinquin[56], an immense number of probes are introduced to the literature which are important for the biological systems.

In our second project, we aimed to synthesize a novel fluorescent sensor, which will be used in the sensing of the zinc ions.Our starting material was 2, 4-lutidine which was commercially available. In order to functionalize the core of this molecule, we first conducted a protection reaction on the core ring. Then, acetylation reaction on the C-2 carbon followed by the oxidation on C-4 carbon yielded our aldehyde. After we synthesized our BODIPY core we were able to purify and characterize it through NMR spectra. As a future work, we will aim to functionalize it on the pyridine ring, which will then give a final step with N-methyl-1-(pyridin-2-yl) methanamine to yield our final molecule.

As previously mentioned, anions and cations have large concentrations in biological systems since each of them is responsible for different part and their presence is required for the smooth operation of the biological systems. Our final molecule as shown in **Figure 41,** coordinated to zinc cations, is expected to be the one of the many examples of the fluorescent sensors.

In biological systems, the zinc cations are expected to coordinate through the amine moieties as shown. As a result, our molecule will be able to detect the presence of the cation. Once the zinc molecule

is coordinated to the molecule, there is a photo induced electron transfer between two moieties. Here, the zinc cation acts as the electron donor and the BODIPY molecule acts as the electron acceptor unit.

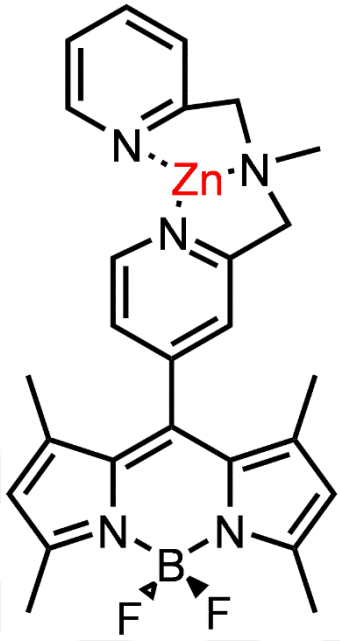

Figure 41: Structure of the Target molecule.

As a further work, our molecule can be further used to investigate the presence of hyper phosphorylated tau proteins. Tau proteins are known to stabilize microtubules in the brain cells. In the case of brain diseases like Alzheimer disease, this proteins become defective and can no longer stabilize microtubules properly. Hyperphosphorylation phenomenon is the cause of the tau proteins to tangle each other. As a result of this, the diagnosis of Alzheimer's disease can be observed through the presence of different hyperphosphorylated tau proteins in brain cells. Inspired by the work by Hamachi and his coworkers[60], after the binding of the Zinc cation on our target molecule, the presence of various hyper phosphorylated tau proteins can further be examined.

CHAPTER 4: CONCLUSION

In the first part of this thesis, we aimed to achieve a chemical control over the thermolysis of an endoperoxide to give singlet oxygen. For this purpose, we were able to synthesize and purify the 1, 4-dimethyl naphthalene based endoperoxide which was protected on the hydroxide group at C-2, molecule 29. Each step was characterized by ^{1}H NMR and ^{13}C NMR spectra, and we were able to purify all of the molecules that are synthesized.

Our target was to have a molecule that releases singlet oxygen at a slow rate at room temperature. Then, upon deprotonation in the presence of fluoride anion, we expected a much faster rate than the initial molecule. In order to understand this phenomenon, we used the help of the absorbance and fluorescence measurements. Change in absorption spectra showed that we were able to generate singlet oxygen with the molecule 29.

As a future work, our final endoperoxide may serve as a source of singlet oxygen in biological systems. Since initiating apoptosis in singlet oxygen plays a huge role on many areas like photodynamic therapy of cancer cells or sensing in living organisms, our work has promising results for the future development of these concepts.

In the second part of this thesis, we aimed to synthesize a novel fluorescent sensor which is a derivative of a BODIPY dye. We were able to synthesize the first step of the BODIPY molecule and purify it. After some further reactions, this molecule will bear a picolyl amine derivative moiety on the meso position. It is then expected to work as a sensor molecule for Zn^{2+} cations and generate a photoinduced charge transfer.

With the light of our results and the previously done research on this topic, our target molecule may play a role in the future, on the sensing of hyperphosporylated tau proteins which are recognized to be produced in the brain of patients with Alzheimer's disease.

BIBLIOGRAPHY

[1] H. Wasserman, D. Larsen, “Formation of 1, 4 Endoperoxides from the Dye- sensitized Photo-oxygenation of Alkyl-naphthalenes,” *J. of The Chem. Soc. Chem. Comm*, no.5, pp. 253-254, 1972.

[2] A.U. Khan, M. Kasha, "Red Chemiluminescence of Molecular Oxygen in Aqueous Solution,"*J. Chem Phys*, vol. 39, no.8, pp. 2105, 1963.

[3] M.C. De Rosa, R.J.Crutchley, "Photosensitized singlet oxygen and its applications," *Coord. Chem Rev*, vol. 233-234, pp. 351-371, 2002.

[4] T.P. Devasagayam, J.P. Kamat, "Biological significance of singlet oxygen," *Indian J. Exp Biol*, vol. 40, pp. 680-692, 2002.

[5] J.R. Kanofsky, "Singlet oxygen production by biological systems," *Chem Biol Interact*, vol.70 no.1-2, pp. 1-28, 1989.

[6] I. E. Kochevar, “Singlet Oxygen Signaling: From Intimate to Global,” *Science's STKE*, vol. 221, pp. 7, 2004.

[7] S.J. Andrasik, "Singlet Oxygen Generation Using New Fluorene-Based Photosensitizers Under One- and Two-Photon Excitation," *Dissertation*. 2007.

[8] O. Günther, K. Ziegler, "Die Synthese des Ascaridols," *The Science of Nature*, vol. 32, no. 14, pp. 157-158, 1944.

[9] C. Dufraisse, E. S., "Photooxydation sur Cycle Pentagonal: Photooxydiphenylisobenzofuran," *Comptes Rendus Chimie*, vol. 223, pp. 735-737, 1946.

[10] C. Jacquot, "Cycloadditions with Singlet Oxygen Mechanism and Substituent Directing Effects," Reported by Cyril Jacquot, pp. 17-24, 1968.

[11] S. Atilgan, Z. Ekmekci, L. Dogan, D. Guc, E.U. Akkaya, "Water soluble distyryl-boradiazaindacenes as efficient photosensitizers for photodynamic therapy," *Chem Commun*, vol.42, pp. 4398-4400, 2006.

[12] C. Moureu, C. Dufraisse, P. Dean, "An organic peroxide separable from the rubrene peroxide," *C. R. Hebd. Seances. Acad. Sci*, vol. 182, pp. 1584–1587, 1926.

[13] J.M. Aubry, C Pierlot, J. Rigaudy, R.Schmidt, "Reversible binding of oxygen to aromatic compounds," *Acc. Chem. Res*, vol. 36, no.9, pp. 668-675, 2003.

[14] I. Saito, T. Matsuura, K. Inoue, "Formation of superoxide ion from singlet oxygen. Use of a water-soluble singlet oxygen source," *J. Am. Chem. Soc*, vol.18, pp. 188-190, 1981.

[15] W. Nieuwint, J.M. Aubry, F. Arwert, H. Kortbeek, S. Herzberg, H. Joenje, "Inability of chemically generated singlet oxygen to break the DNA backbone," *Free Radic. Res. Commun*, vol.1, no.1, pp. 1-9, 1985.

[16] I. Saito, R. Nagata, H. Nakagawa, H. Moriyama,T. Matsuura, K. Inoue, "New singlet oxygen source and trapping reagent for peroxide intermediates," *Free Rad Res Comms*, vol.2, pp. 327-336, 1987.

[17] C. Foote, "Mechamsm of Addition of Singlet Oxygen To Olefins and Other Substrates," *Pure Appl. Chem*, vol.27, no. 4, pp. 635-646, 1971.

[18] A. J. Bloodworth, "Endoperoxides In Singlet O_2," Boca Raton: Florida, 1985.

[19] M.Balci, "Bicyclic Endoperoxides and Synthetic Applications," *Chem. Rev*, vol. 81, pp. 91-108, 1981.

[20] P. Atkins and J. de Paula. "Physical Chemistry," vol .74, no. 16, pp. 706, 2006.

[21] C. J. M. van den Heuvel, J. W. Verhoeven and, Th. J. de Boer, "A frontier orbital description of the reaction of singlet oxygen with simple aromatic systems," *Recueil des Travaux Chimiques des Pays-Bas*, vol. 99, pp. 280 - 284, 1980.

[22] J-M. Aubry, B. Mandard-Cazin, M. Rougee, R. V. Bensasson, "Kinetic Studies of Singlet Oxygen [4+2] Cycloadditions with Cyclic 1,3 Dienes in 28 Solvents," *J. Am. Chem. Soc*, vol. 117, no. 36, pp. 9159–9164, 1995.

[23] M. Bobrowski, A. Liwo, S. Odziej, D. Jeziorek, T. Ossowski, "CAS MCSCF/CAS MCQDPT2 study of the mechanism of singlet: Oxygen addition to 1,3-butadiene and benzene," *J Am Chem Soc*, vol. 122, no. 34, pp. 8112-8119, 2000.

[24] Ethirajan M., Chen Y., Joshi P., Pandey R.K., "The role of porphyrin chemistry in tumor imaging and photodynamic therapy," *Chem. Soc. Rev*, vol. 40, no.1, pp. 340-362, 2011.

[25] N.J.Turro, M. Chow, J. Rigaudy, "Mechanism of Thermolysis of Endoperoxides of Aromatic Compounds. Activation Parameters, Magnetic Field, and Magnetic Isotope Effectst," *J. Am Chem. Soc*, vol.103, no. 4, pp. 7218-7224, 1981.

[26] L.Slavětínská, J. Mosinger, P. Kubát, "Supramolecular carriers of singlet oxygen: Photosensitized formation and thermal decomposition of endoperoxides in the presence of cyclodextrins," *J. Photochem .Photobiol. A Chem*, vol.195, no.1, pp. 1-9, 2008.

[27] C. Pierlot, S. Hajjam, C. Barthmy, J.Aubry, "Water-soluble naphthalene derivatives as singlet oxygen (102 , lag) carriers for biological media," *Source*, vol.36, pp. 31-39, 1996.

[28] V. Nardello, D. Brault, P. Chavalle, J.M. Aubry. "Measurement of photogenerated singlet oxygen ($^1O_2$ ($^1\Delta(g)$)) in aqueous solution by specific chemical trapping with sodium 1,3-cyclohexadiene-1,4-diethanoate," *J. Photochem. Photobiol. B Biol*, vol. 39, no. 2, pp.146-155, 1997.

[29] E. Skovsen, J.W. Snyder, J.D.C. Lambert, P.R. Ogilby, "Lifetime and diffusion of singlet oxygen in a cell," *J. Phys. Chem. B*, vol. 109, no. 18. pp. 8570-8573, 2005.

[30] M.J.Steinbeck, U.Khan, M.J. Karnovsky, "Intracellular singlet oxygen generation by phagocytosing neutrophils in response to particles coated with a chemical trap," *J. Biol. Chem*. vol. 267, no.19, pp. 13425-13433, 1992.

[31] S. Hatz, J.D.C. Lambert, P.R. Ogilby, "Measuring the lifetime of singlet oxygen in a single cell: addressing the issue of cell viability," *Photochem. Photobiol. Sci*, vol. 6, no.10, pp. 1106-1116, 2007.

[32] J-L. Ravanat, T. Douki T, P. Duez, "Cellular background level of 8-oxo-7,8-dihydro-2'-deoxyguanosine: an isotope based method to evaluate artefactual oxidation of DNA during its extraction and subsequent work-up," *Carcinogenesis*, vol. 23, no.11, pp. 1911-1918, 2002.

[33] S. Kim, T. Tachikawa, Fujitsuka M, Majima T. "Far-red fluorescence probe for monitoring singlet oxygen during photodynamic therapy," *J. Am. Chem. Soc*, vol. 136, no.33, pp. 11707-11715, 2014.

[34] P.G.M.Wuts, "Greene's Protective Groups in Organic Synthesis: Fifth Edition." *Greene's Prot Groups Org. Synth Fifth Ed*, pp. 1-1360, 2014.

[35] A. D'Sa B, D. McLeod, J.G.Verkade, "Nonionic superbase-catalyzed silylation of alcohols," *J. Org Chem*, vol. 62. no.15, pp. 5057-5061, 1997.

[36] E.J. Corey, A.Venkateswrlu, "Protection of Hydroxyl Groups as tert-Butyldimethylsilyl Derivatives," *J. Am. Chem. Soc*, vol. 94, pp. 6190-6191, 1972.

[37] P. Patschinski, C. Zhang, H. Zipse, "Supplemental Information for The Lewis Base-Catalyzed Silylation of Alcohols — A Mechanistic Analysis Table of Contents" pp.1-185, 2014.

[38] P. Anzenbacher, K. Jursikov, J.L. Sessler, "Second generation calixpyrrole anion sensors," *J. Am. Chem. Soc*, vol.122, no.38, pp. 9350-9351, 2000.

[39] G. Xu, M. Tarr, "A novel fluoride sensor based on fluorescence enhancement," *Chem. Commun*, vol. 9, pp. 1050-1051, 2004.

[40] S. Malhotra, T. Kim, Angelica, Y. Fong, " Use of an Oncolytic Virus Secreting GM-CSF as Combined Oncolytic and Immunotherapy for Treatment of Colorectal and Hepatic Adenocarcinomas," *NIH Public Access*. vol. 141, no.4, pp. 520-529, 2008.

[41] I.S. Turan, E.U. Akkaya, "Chemiluminescence Sensing of Fluoride Ions Using a Self Immolative Amplifier," *Org Lett*, vol.16, pp. 1680-1683, 2014.

[42] Z.Yang, K. Zhang, F. Gong, "A new fluorescent chemosensor for fluoride anion based on a pyrrole-isoxazole derivative," *Beilstein J. Org Chem.*, vol. 7, no. 46-52, 2011.

[43] I. Simsek Turan, F. Pir Cakmak, F.Sozmen, "Highly selective fluoride sensing via chromogenic aggregation of a silyloxy-functionalized tetraphenylethylene (TPE) derivative," *Tetrahedron Lett*, vol. 55, no.2, pp. 456-459, 2014.

[44] J.M. Lehn, "Perspectives in supramolecular chemistry - From molecular recognition towards molecular information processing and self-organization," *Angew Chem Int Ed Engl*. vol. 29, no.11, pp. 1304-1319, 1990.

[45] J-M. Lehn, "Design of organic complexing agents Strategies towards properties," *Alkali Met Complexes with Org Ligands*, vol.16, pp. 1-69, 1973.

[46] M. Eigen, L. de Maeyer, "Chemical means of information storage and readout in biological systems," *Naturwissenschaften*, vol. 53, no.3, pp. 50-57, 1966.

[47] J-M. Lehn, "Cryptate inclusion complexes. Effects on solute-solute and solute-solvent interactions and on ionic reactivity," *Pure Appl Chem*. vol 52, no.4, pp. 2303-2319, 1980.

[48] J-M. Lehn, "Supramolecular Chemistra," *Science*, vol. 227, no. 849, 1987.

[49] A.W. Czarnik. "Supramolecular Chemistry, Fluorescence, and Sensing," pp.1-9, 1993.

[50] A. Loudet, K. Burgess, "BODIPY Dyes and Their Derivatives: Syntheses and Spectroscopic Properties," *Chem Rev*, 107(11): 4891-4932, 2007.

[51] "The Jablonski Diagram," *Journal of Photochemistry and Photobiology, B: Biology*, vol. 2, pp. 399 - 408, 1988.

[52] S.R. Andersont, G.Weber, "Evidence for Preferential Orientation of the Ligand," vol.8, no.1, pp. 371-377, 1969.

[53] J.K. Atkinson, W.J. Cranny,W. V. Glasspool, J. Mihell, "Investigation of the performance characteristics and operational lifetimes of multi-element thick film sensor arrays used in the determination of water quality parameters," *Sensors Actuators, B Chem*, vol. 54, no.3, pp. 215-231, 1999.

[54] C.S. De Castro, J. Sergio Seixas De Melo, A. Fernandez-Lodeiro, C.Navirez, C. Lodeiro, "Spectroscopic and photophysical studies of a naphthalene-based emissive probe for metal cations," *Inorg. Chem. Commun*, vol. 47, pp. 27-32, 2014.

[55] W. Putzbach, N.J. Ronkainen. "Immobilization techniques in the fabrication of nanomaterial-based electrochemical biosensor: a review," *Sensors (Basel)*, vol. 13, no. 4, pp. 4811-4840, 2013.

[56] K. P. Carter, A. M.Young, A. E. Palmer, "Fluorescent sensors for measuring metal ions in living systems," *Chem. Rev*, vol. 114, no.8, pp. 4564-4601, 2014.

[57] Y. Wu, X. Peng, B. Guo et al, "Boron dipyrromethene fluorophore based fluorescence sensor for the selective imaging of Zn(II) in living cells," *Org Biomol Chem*, vol. 3(c), pp. 1387-1392, 2005.

[58] S. Zhu, J. Zhang, J. Janjanam, "Highly water-soluble BODIPY-based fluorescent probes for sensitive fluorescent sensing of zinc(ii)," *J. Mater. Chem. B*, vol. 1, no. 12, pp. 1722-1728, 2013.

[59] S.Niu, "Advanced water soluble BODIPY dyes: Synthesis and application," vol. 82, 2011.

[60] A. Ojida, T. Sakamoto, M. Inoue, S. Fujishima, G. Lippens, I. Hamachi, "Fluorescent BODIPY-Based Zn (II) Complex as a Molecular Probe for Selective Detection of Neurofibrillary Tangles in the Brains of Alzheimer's Disease Patients," *J. Am. Chem. Soc*, vol. 131, no. 18, pp. 6543-6548, 2009.

[61] B. Daly, J. Ling, A. P. de Silva, "Current developments in fluorescent PET (photoinduced electron transfer) sensors and switches," *Chem Soc Rev*, vol.44, pp. 4203-4211, 2015.

[62] Y. Jiao, B. Zhu, J. Chen , X. Duan, "Fluorescent sensing of fluoride in cellular system," *Theranostics*, vol. 2, pp. 173-187, 2015.

[63] Y.Suzuki, K. Yokoyama, "Development of functional fluorescent molecular probes for the detection of biological substances," *Biosensors*, vol.5, no.2, pp. 337-363, 2015.

[64] E.N. Ushakov, M. V. Alfimov, S.P. Gromov, "Crown ether-based optical molecular sensors and photocontrolled ionophores," *Macroheterocycles*, vol. 3 no.4, pp. 189-200, 2010.

[65] P. H. Service, "Copper(II) Halides. The Synthesis," vol. 35, no. 10, pp. 3436-3442, 1970.

[66] A.K. Sharma, S. Amin, S. Kumar, "An Abbreviated Synthesis of 7,12-Dimethylbenz[a]anthracene and Benzo[c]chrysene Metabolites Using the Suzuki Reaction," *Polycycl. Aromat. Compd*, vol. 22, no.3-4, pp. 277-288, 2002.

[67] M. Jiang, H-J. Yang, Y. Li, Z-Y. Jia, H. Fu, "Metal-free synthesis of substituted phenols from arylboronic acids in water at room temperature," *Chinese Chem Lett*, vol. 25, no.5, pp. 715-719, 2014.

[68] V. Blechta, S. Abata, J. Sukora, J. Hetflej, L. Soukupov, J. Schraml, "The effect of solvent accessible surface on Hammett-type dependencies of infinite dilution ^{29}Si and ^{13}C NMR shifts in ring substituted silylated phenols dissolved in chloroform and acetone," *Magn. Reson. Chem*, vol. 50, no.2, pp. 128-134, 2012.

[69] R. Glaucia Martinez, J.-L. Ravanat, "Synthesis of a Naphthalene Endoperoxide as a Source of ^{18}O-labeled Singlet Oxygen for Mechanistic Studies," *J. Am. Chem. Soc*, vol. 122, pp. 10212-10213, 2000.

[70] J. Bartelmess and W. Weare, "Preparation and characterization of multi-cationic BODIPYs and their synthetically versatile precursors," *Dye Pigment*, vol. 97, no.1, pp. 1-8, 2013.

APPENDIX A: ^{1}H NMR and ^{13}C NMR SPECTRA

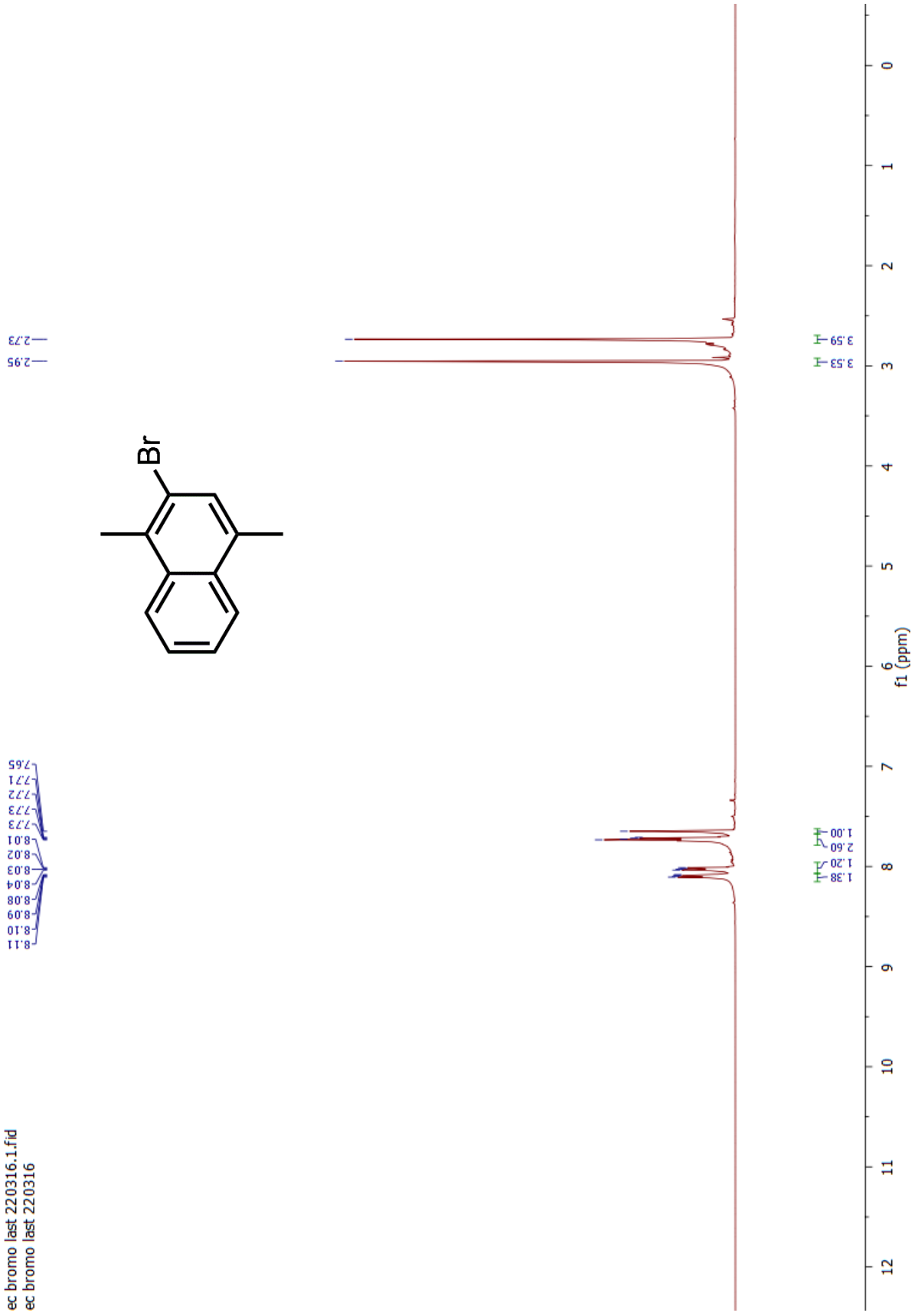

Figure 42: ^{1}H-NMR spectrum of Compound 36.

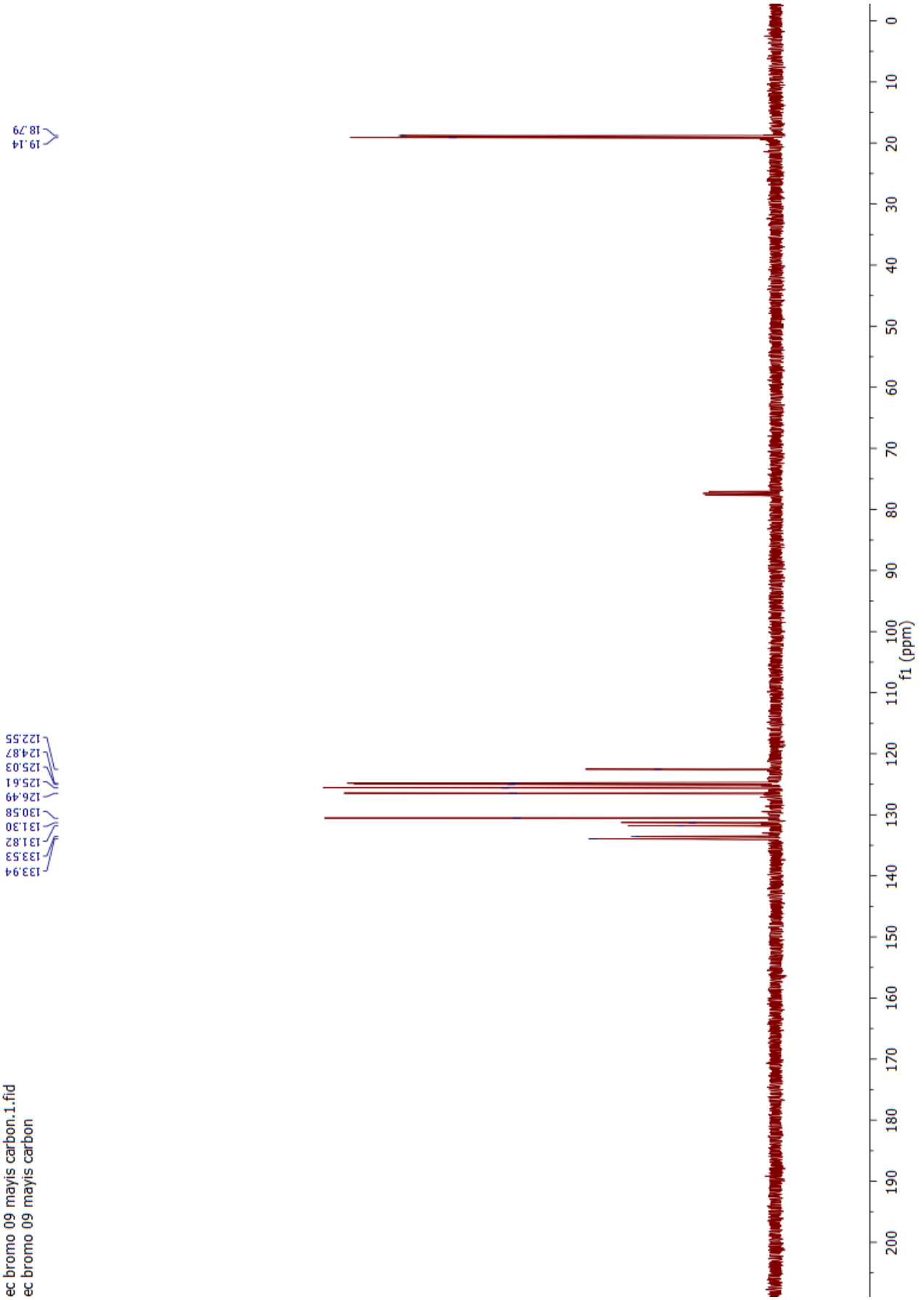

Figure 43: ^{1}C-NMR spectrum of Compound 36.

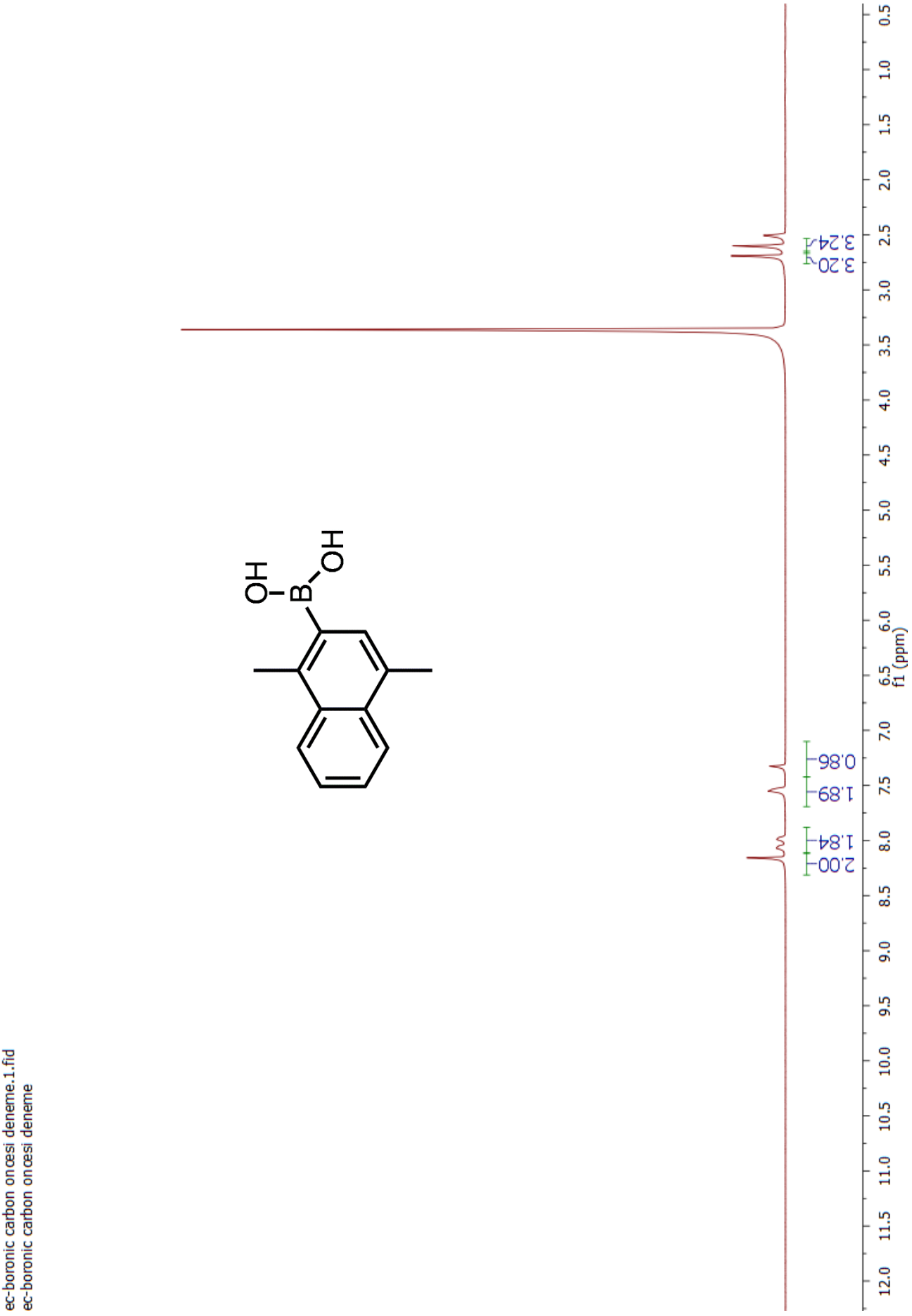

Figure 44: ^{1}H-NMR spectrum of Compound 37.

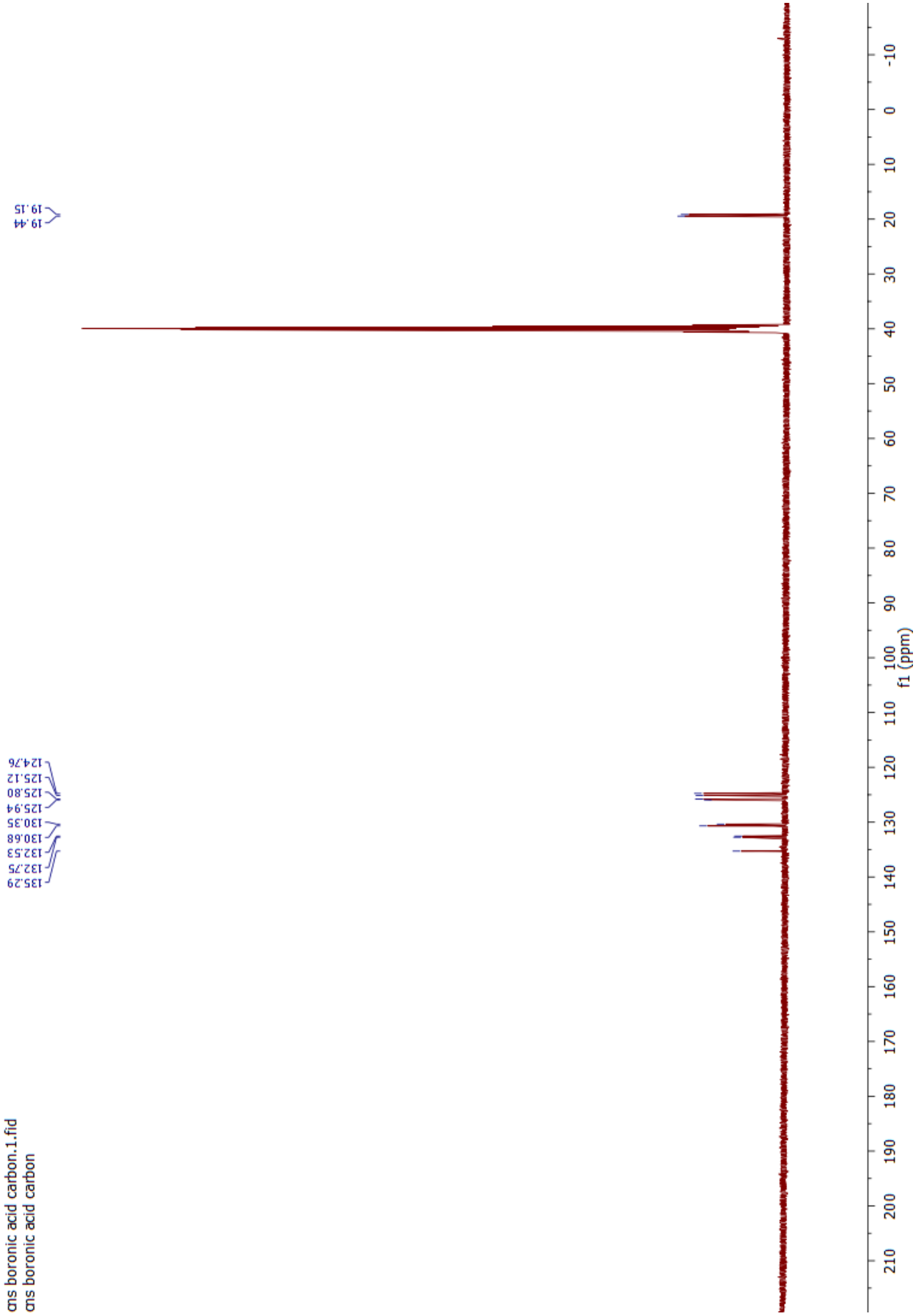

Figure 45: [1]C-NMR spectrum of Compound 37.

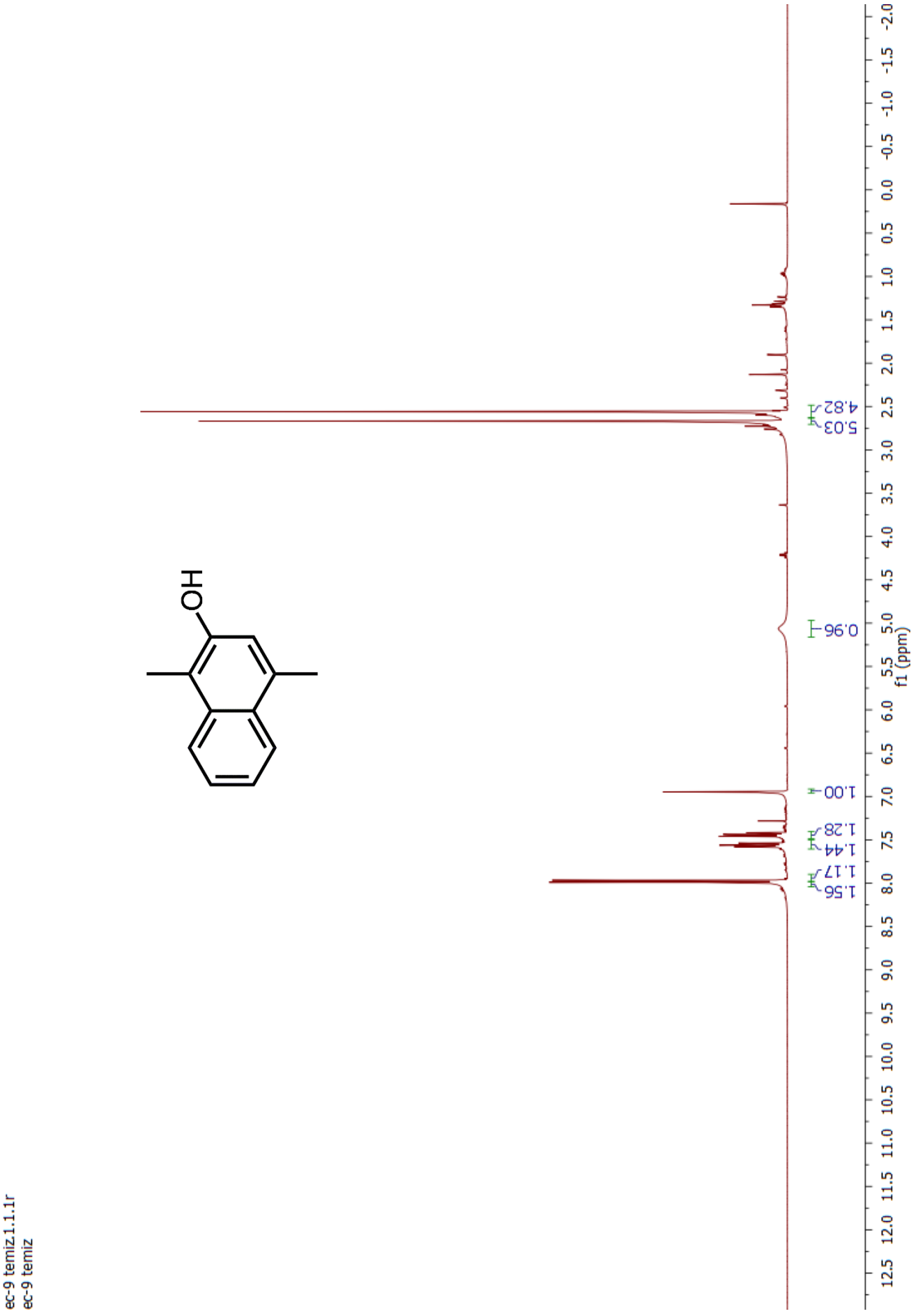

Figure 46:[1]H-NMR spectrum of Compound 38.

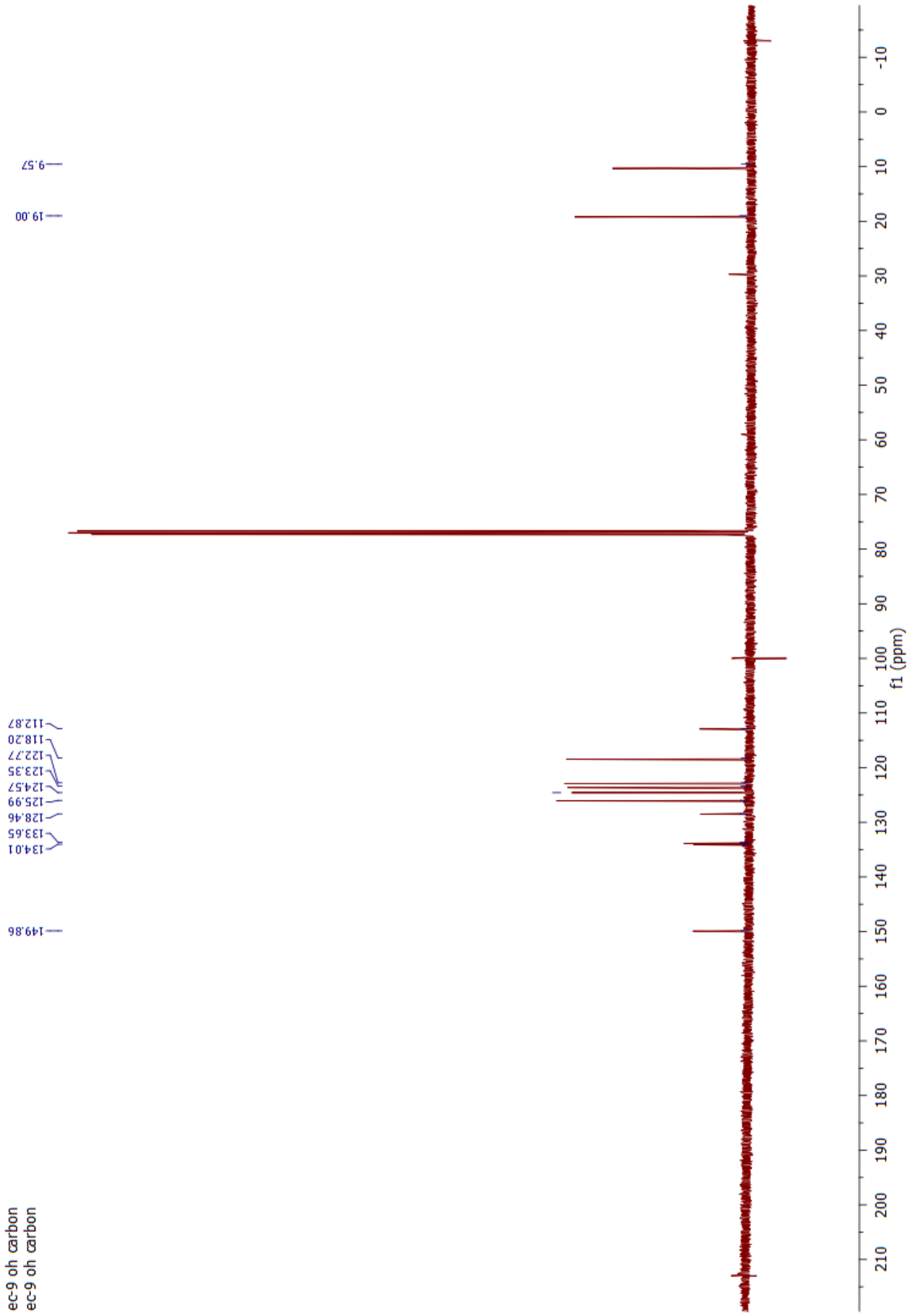

Figure 47: ^{13}C-NMR spectrum of Compound 38.

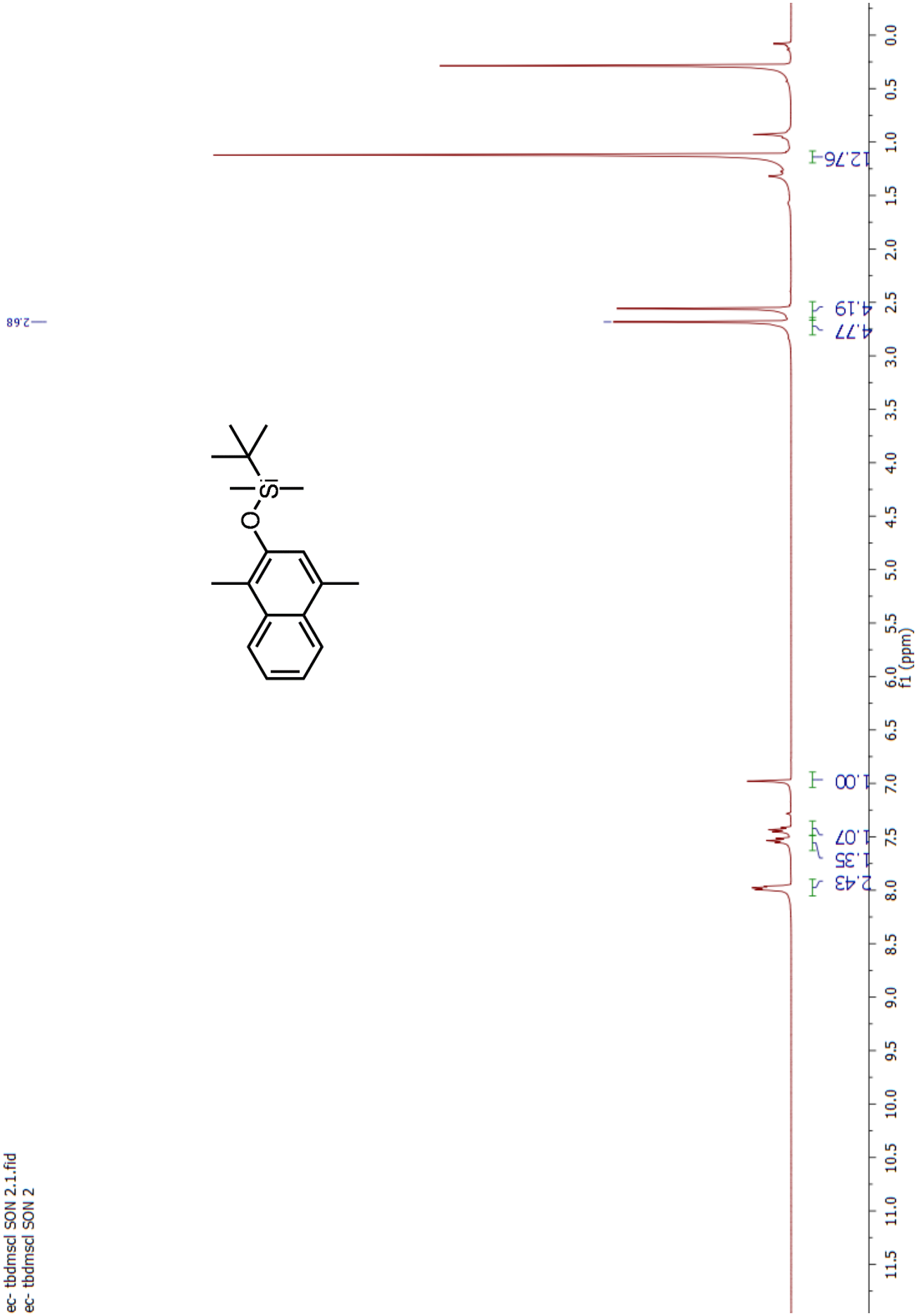

Figure 48: ^{1}H-NMR spectrum of Compound 39.

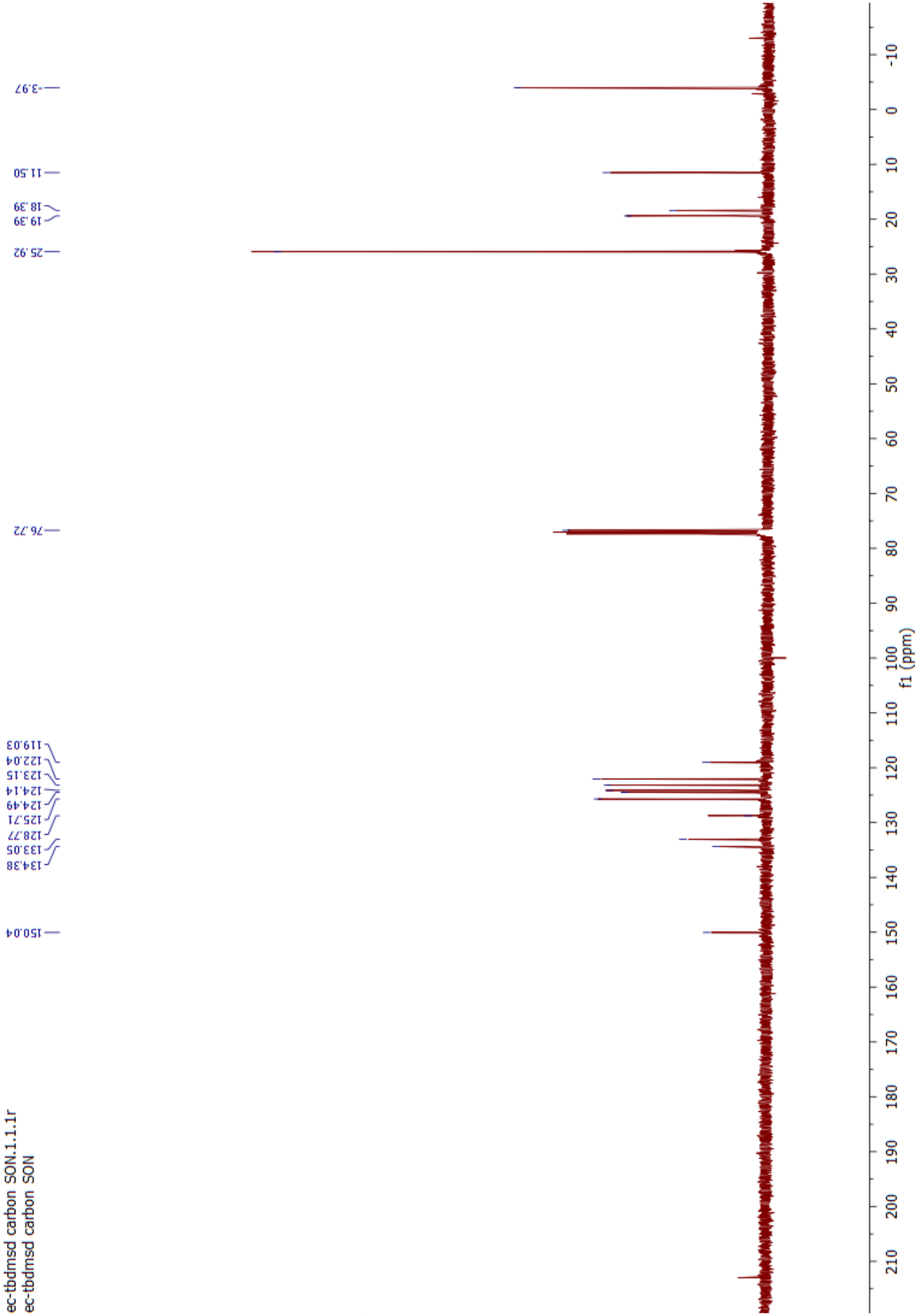

Figure 49: ^{13}C-NMR spectrum of Compound 39.

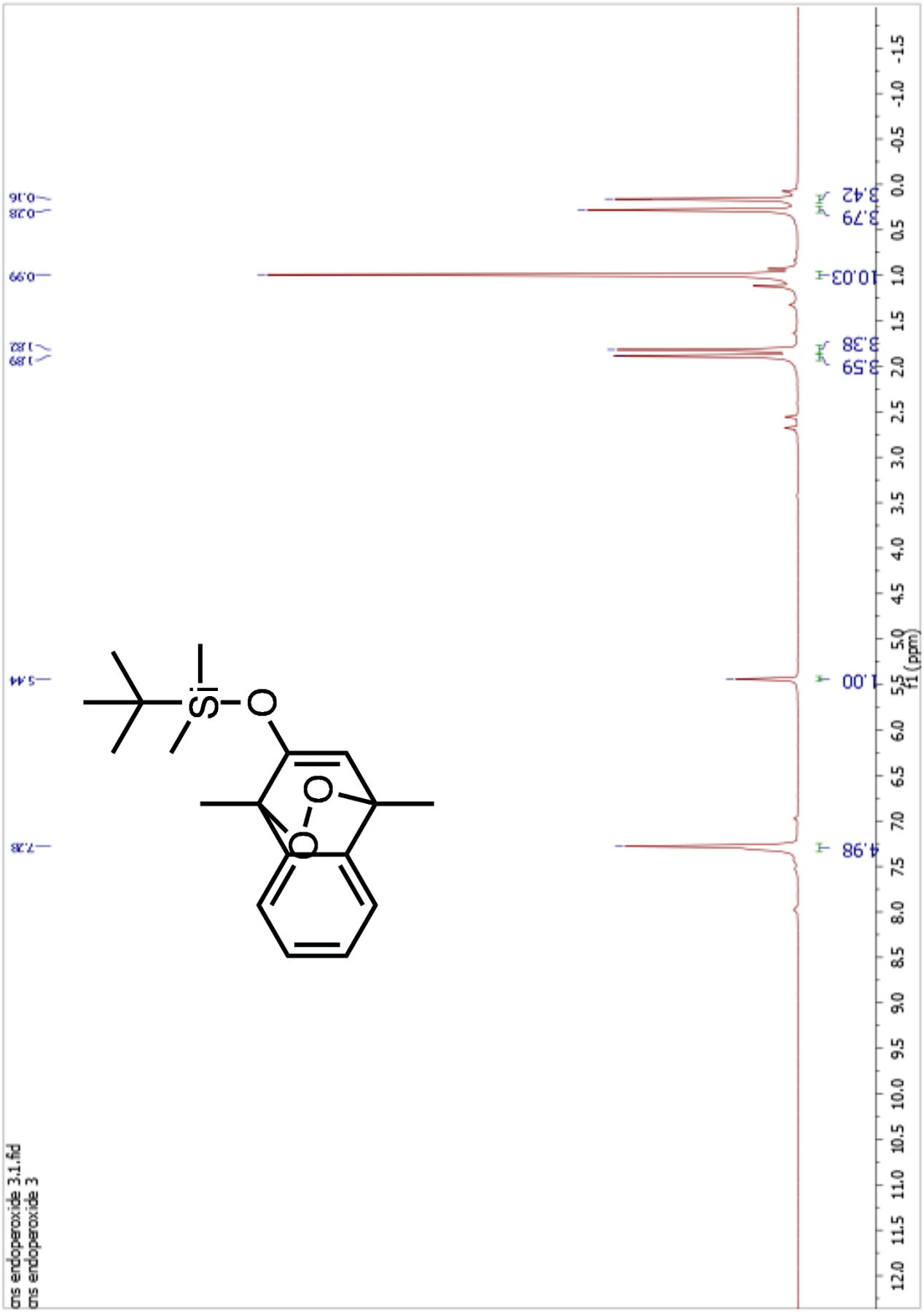

Figure 50: ^{1}H-NMR spectrum of 40.

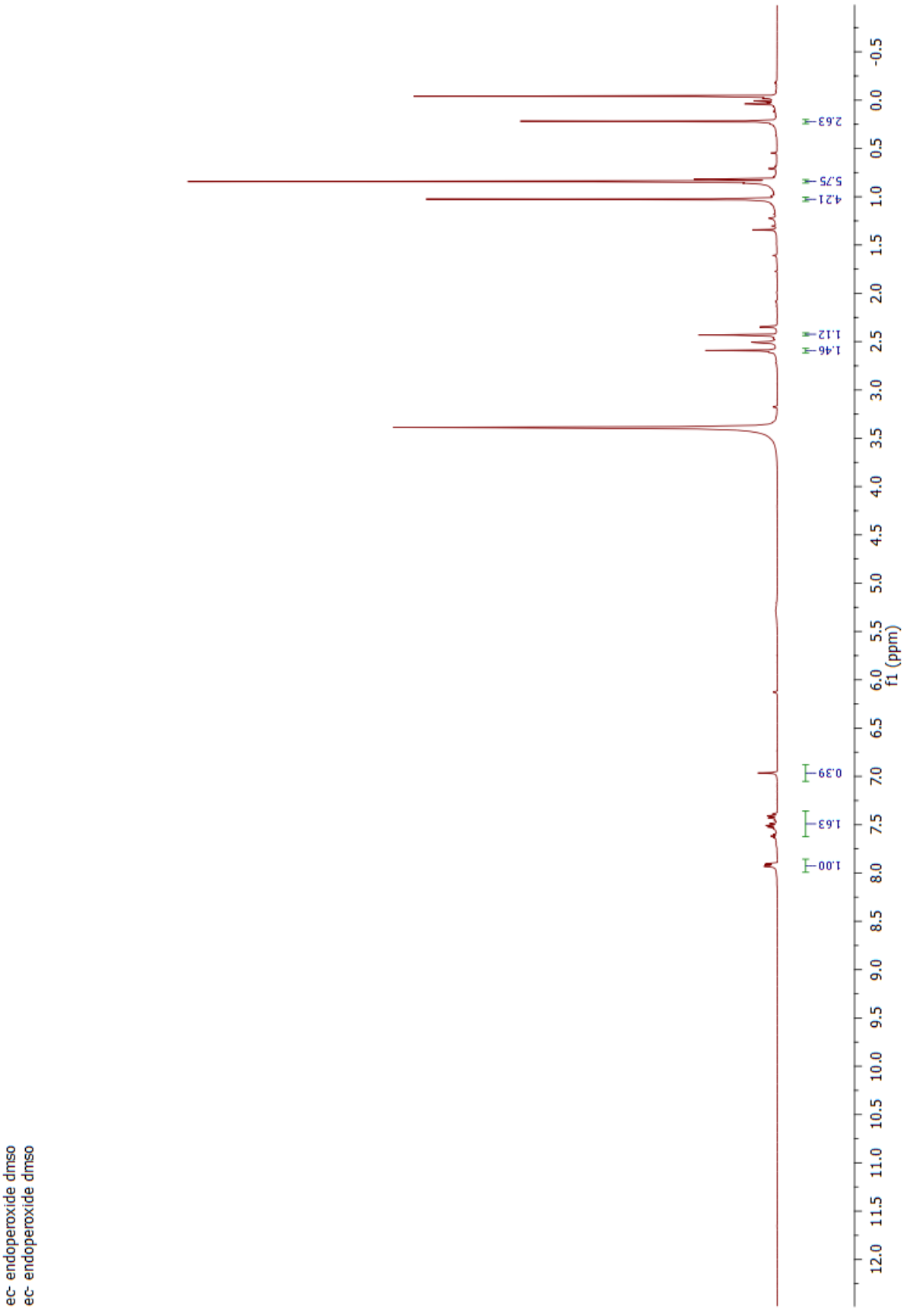

Figure 51: ^{1}H-NMR spectrum of Compound 40 in $(CD_3)_2SO$.

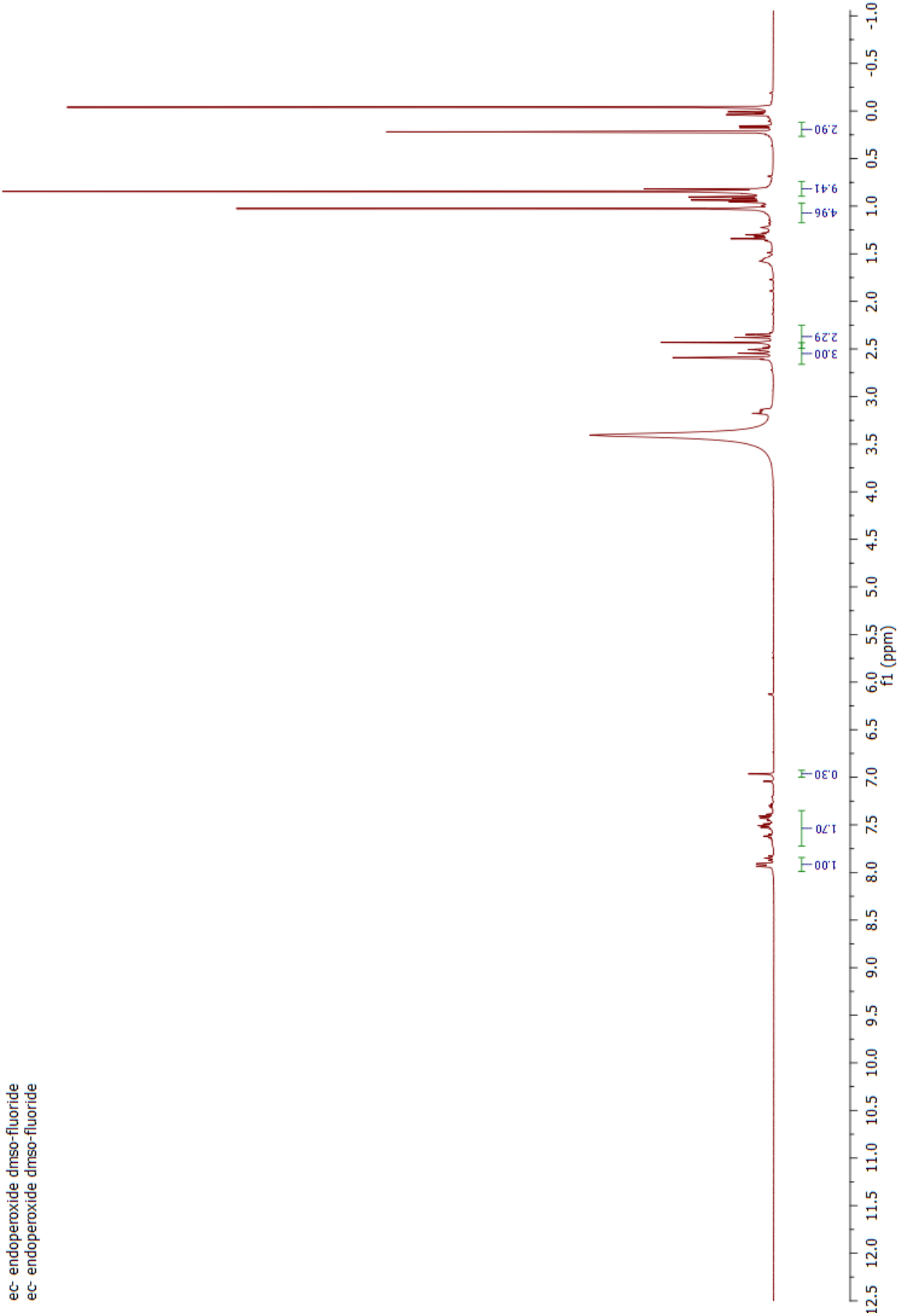

Figure 52: ^{1}H-NMR spectrum of Compound 40 in $(CD_3)_2SO$ with Fluoride anion.

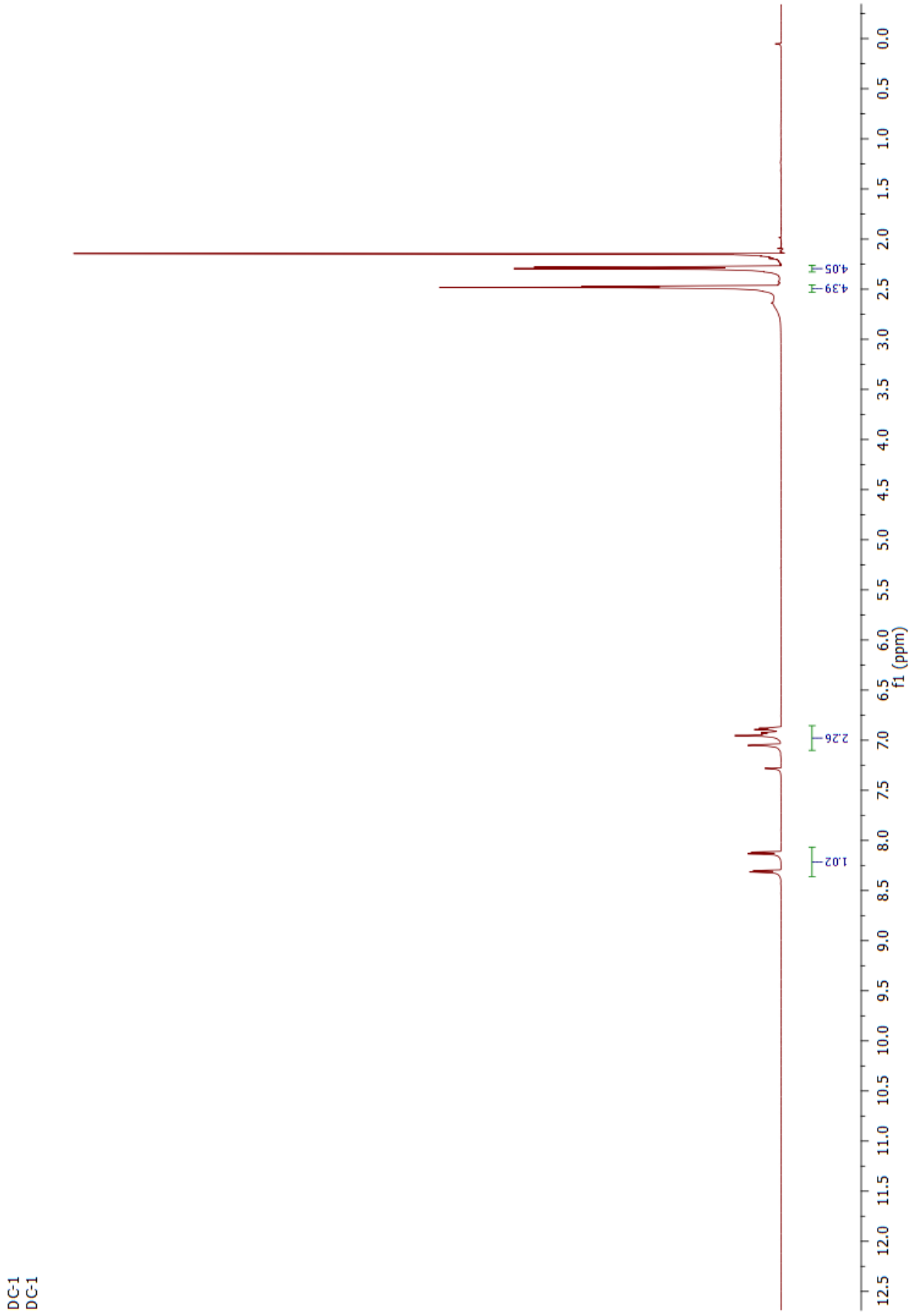

Figure 53: ^{1}H-NMR spectrum of Compound 41.

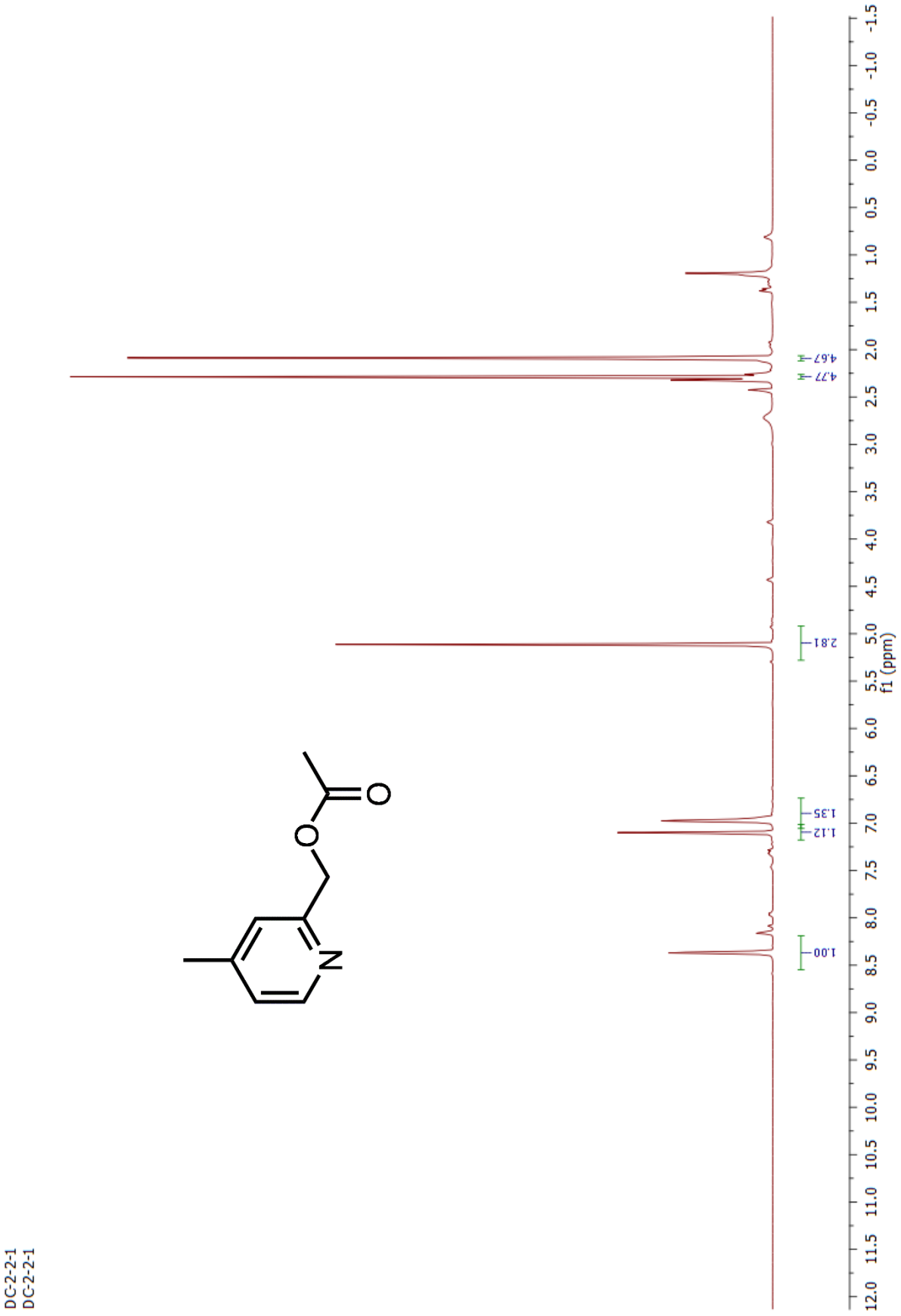

Figure 54: ^{1}H-NMR spectrum of Compound 42.

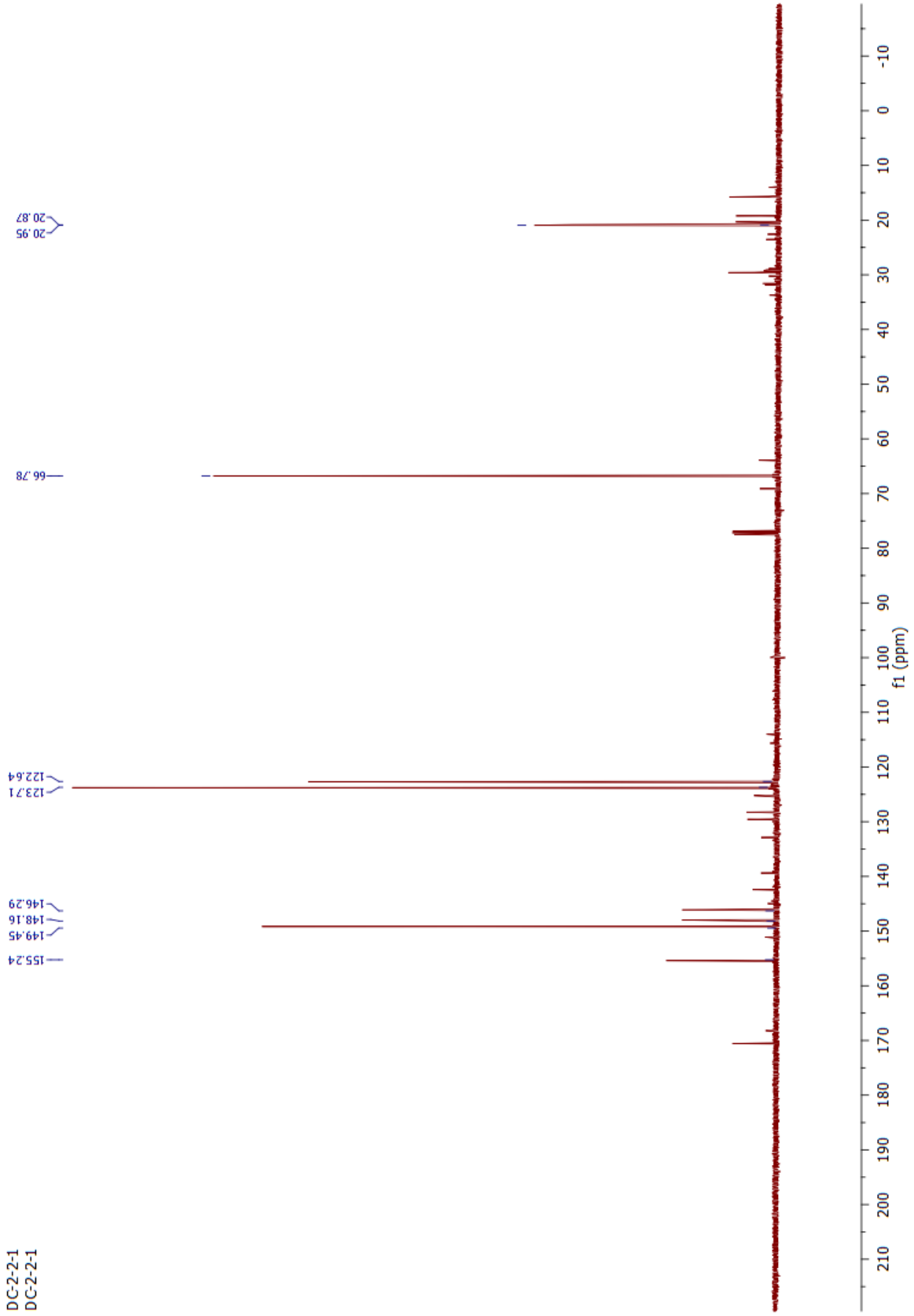

Figure 55: ^{13}C-NMR spectrum of Compound 42.

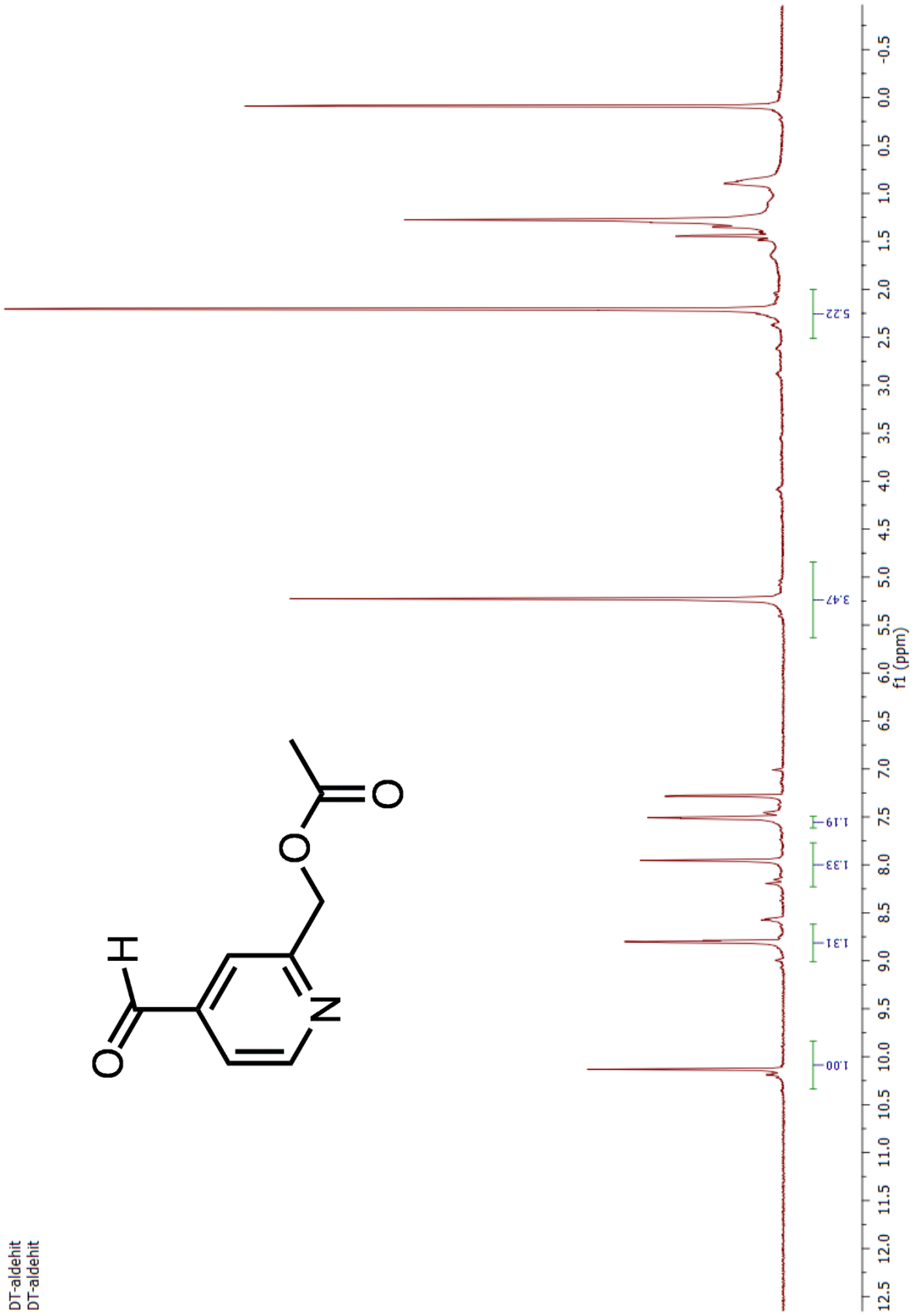

Figure 56: ^{1}H-NMR spectrum of Compound 43.

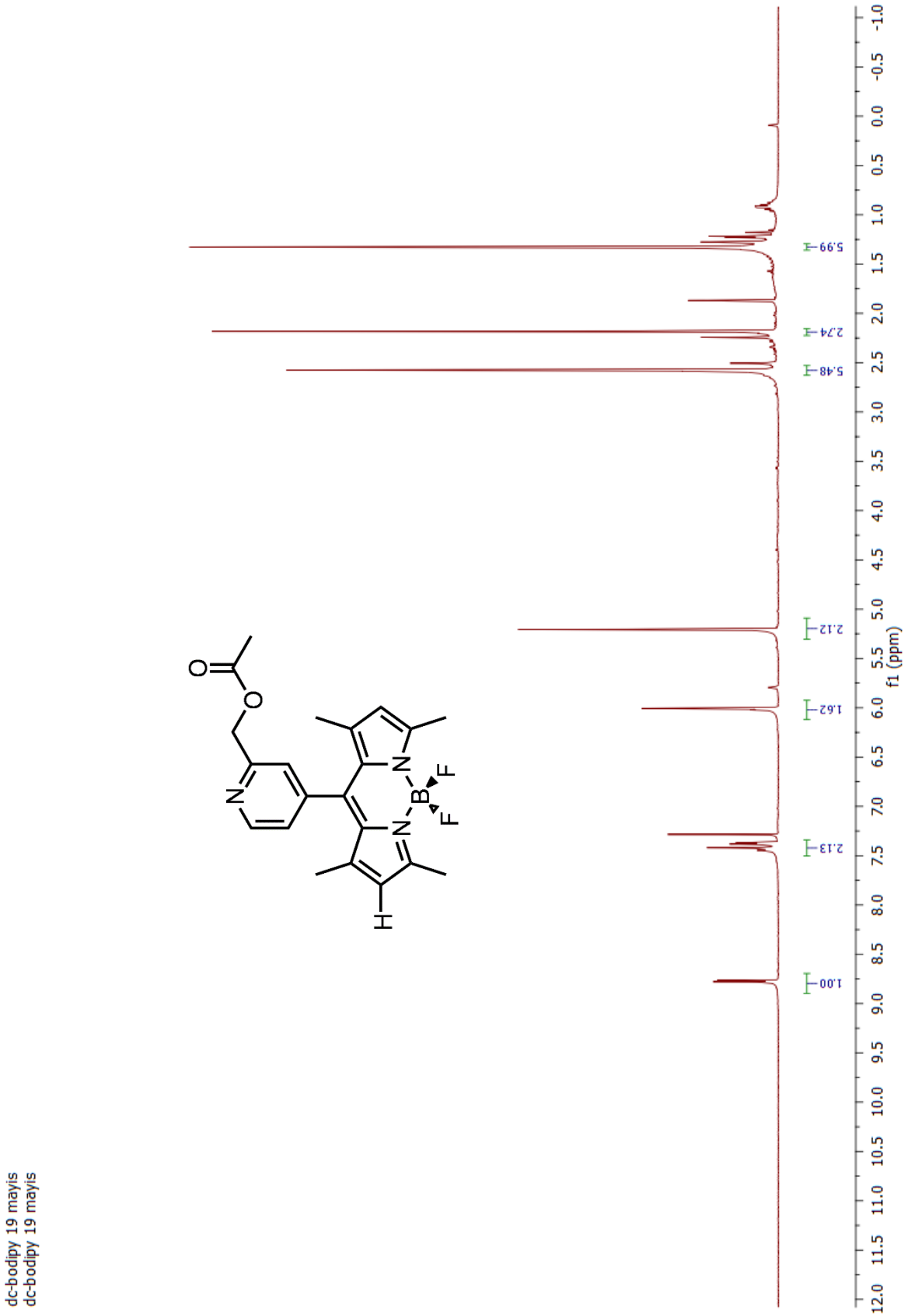

Figure 57: ^{1}H-NMR spectrum of Compound 44.

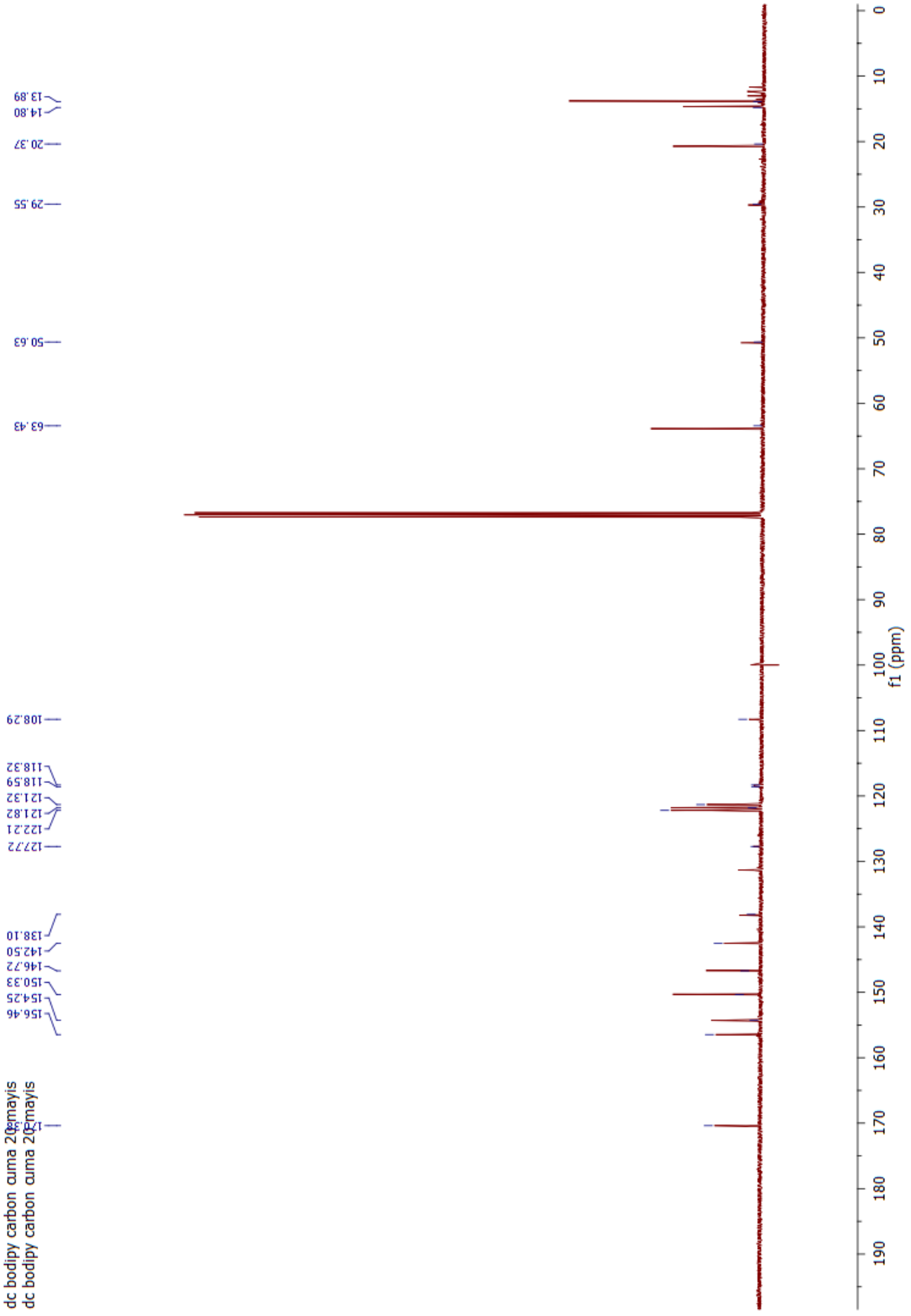

Figure 58: ^{13}C-NMR spectrum of Compound 44.

APPENDIX B: MASS SPECTRA

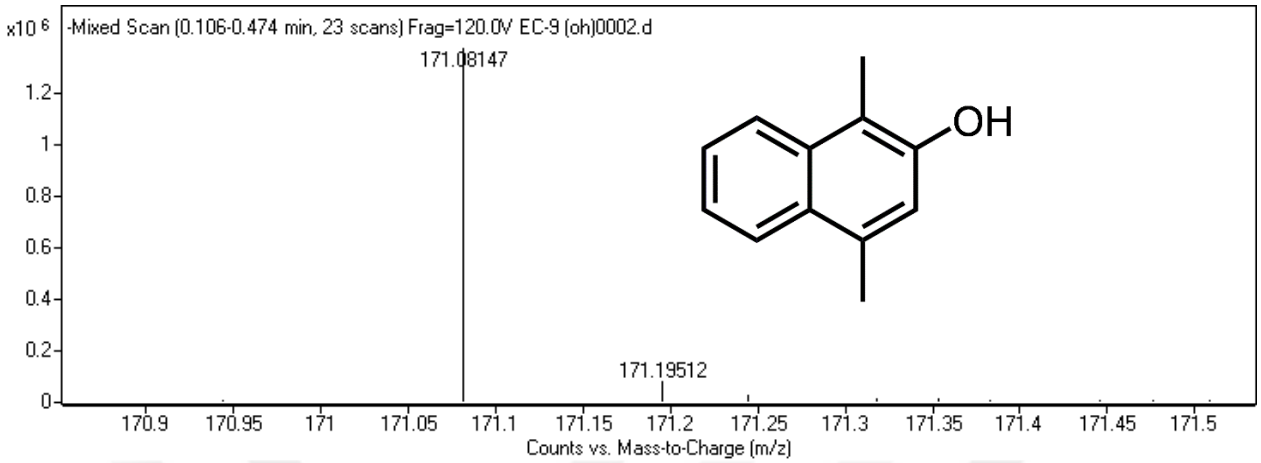

Figure 59: Mass spectrum of Compound 38.

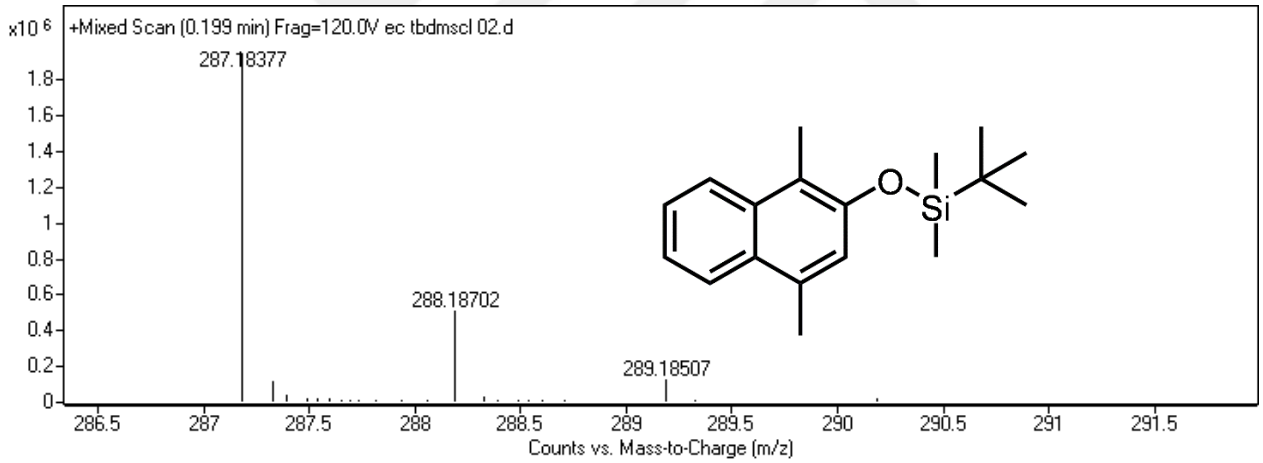

Figure 60: Mass spectrum of Compound 39.

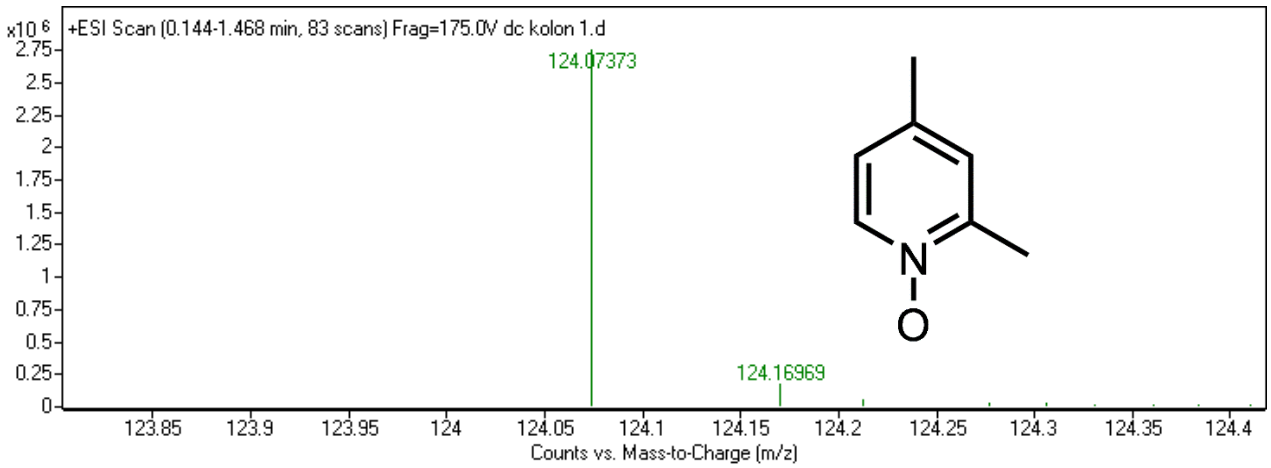

Figure 61: Mass spectrum of Compound 41.

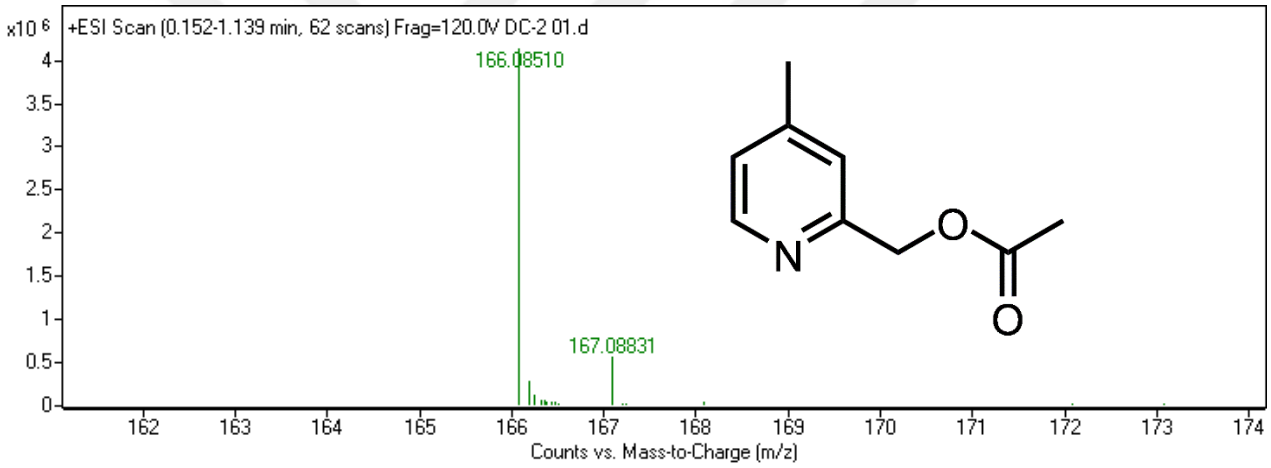

Figure 62: Mass spectrum of Compound 42.

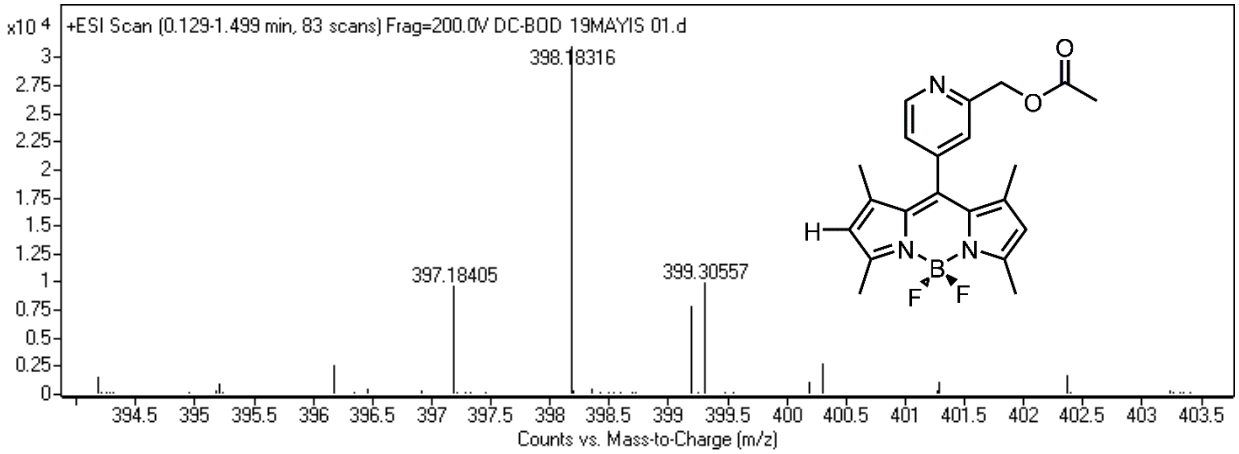

Figure 63: Mass spectrum of Compound 44.